Electronic Supplementary Information for

Photo-induced mitochondrial DNA damage and NADH depletion by -NO_2 modified Ru(II) complexes

Shuang Qi,‡[ab] Zhihui Jin,‡[ab] Yao Jian, [ab] Yuanjun Hou,[a] Chao Li,[a] Yao Zhao,*[c] Xuesong Wang,*[ab] Qianxiong Zhou*[a]

[a] *Key Laboratory of Photochemical Conversion and Optoelectronic Materials, Technical Institute of Physics and Chemistry, Chinese Academy of Sciences, Beijing 100190, P. R. China. Fax: +86-10-62564049; Tel: +86-10-82543592;*

[b] *University of Chinese Academy of Sciences, Beijing 100049, P. R. China;*

[c] *CAS Key Laboratory of Analytical Chemistry for Living Biosystems, Institute of Chemistry, Chinese Academy of Sciences, Beijing 100190, P.R. China.*

E-mail: yaozhao@iccas.ac.cn (Y. Zhao), xswang@mail.ipc.ac.cn (X.Wang); zhouqianxiong@mail.ipc.ac.cn (Q. Zhou).

Experimental section

Materials

All reagents and solvents were obtained from commercial sources, and were used as received. Dichloro(benzene)ruthenium (II) dimer, 1,10-phenanthroline-5,6-dione, benzaldehyde, 4-methoxybenzaldehyde, 4-nitrobenzaldehyde, 2,4-dinitrobenzaldehyde, ammonium acetate, cis-dichlorodiamineplatinum (II), carbonyl cyanide chlorophenyl hydrazine (CCCP) were obtained from Acros. 3-(4,5-dimethylthiazol-2-yl)-2,5-diphenyl-tetrazolium bromide (MTT) was purchased from Alfa Aesar. Calf thymus DNA (CT-DNA), gel loading buffer, and tris-hydroxymethyl-aminomethane (Tris base) were purchased from Sigma Aldrich. Annexin V-FITC/PI apoptosis detection kit, Calcein-AM/PI double staining kit, nuclear and mitochondrial extraction kits were purchased from Solarbio. Dulbecco's modification of Eagle's medium (DMEM), penicillin & streptomycin, and fetal bovine serum (FBS) were purchased from Corning.

Instruments

^{1}H nuclear magnetic resonance (^{1}H NMR) spectra were performed on a Bruker DMX-400 MHz spectrometer. All chemical shifts were given relative to tetramethylsilane (TMS). High-resolution ESI mass spectrometry (HR ESI-MS) spectra were obtained on a Bruker APEX IV (7.0 T) FT_MS. UV-vis absorption spectra were determined on a Shimadzu UV-1601 spectrophotometer. An LED lamp (470 ± 10 nm) was used as a light source for one-photon assays. The two-photo absorption (TPA) cross sections were obtained by the two-photon excited fluorescence (TPEF) method with a Ti: sapphire femtosecond laser system (600-2600 nm, 1000 Hz, 25 fs) as the light source. The absorbance data of the MTT assays were performed on a Thermo MK3 Multiscan microplate reader at 570 nm. HPLC analysis was recorded on an HITACHI series instrument using a WH-C–18 column (5 μm, 4 mm × 150 mm).

Methods

DNA binding constant measurement

The CT-DNA was added in PBS (5 mM, pH 7.4), and was stirred overnight in an ice bath to obtain a clear CT-DNA solution. The CT-DNA concentration was quantified by measuring the extinction coefficient at 260 nm (ε = 6600 M^{-1} cm^{-1}). The DNA binding constants of **Ru-1**-**Ru-4** were measured by CT-DNA titration, and were calculated according to the following formula: [1]

$$(\varepsilon_a - \varepsilon_f)(\varepsilon_b - \varepsilon_f) = (b - (b^2 - \frac{2K^2 C_t[DNA]}{s}))^{0.5} \Big/ 2KC_t$$

$$b = 1 + KC_t + [DNA]/2s$$

where ε_a is the extinction coefficient of a given DNA concentration, ε_f is the extinction coefficient of the free complex, ε_b is the extinction coefficient of the complex when fully bound to DNA, K is the equilibrium binding constant, C_t is the total complex concentration, [DNA] is the DNA concentration in nucleotides in base pairs, and s is the binding site size.

DNA gel electrophoresis

Supercoiled pBR322 DNA in Tris-acetic acid EDTA buffer (pH 8.0) was incubated with different concentrations of Ru complexes. After 20 minutes of irradiation (470 nm, 27 J/cm^2), the loading buffer was added. The sample was loaded on the agarose gel, run at 80 V for 1 h, and then was stained by EB (1 mg/L H_2O solution) for 0.5 h. After washing with water for 2 times, the gel was imaged with Gel Doc XR system (Bio-Rad). The dark sample without irradiation was carried out in parallel.

Cell lines and culture conditions

All cells lines were obtained from China Infrastructure of Cell Line Resource. The cells (A549, SKOV-3, A549/DDP) were routinely incubated in Dulbecco's modified Eagle's medium (DMEM, 1 g/L glucose, Corning) supplemented with 10% (v/v) fetal bovine serum (FBS, Corning), 100 μg/mL streptomycin, and 100 U/mL penicillin under 5% CO_2 and 95% air at 37 °C in a humidified atmosphere. All the hypoxia experiments were performed with 5% CO_2 and 3% O_2 (N_2 was another gas source to control O_2 partial pressure).

MTT assay

The cytotoxicity of the ruthenium (II) complexes and cisplatin were determined by MTT assay. The cells were seeded in 96-well plates at a density of 1×10^4 cells per well for 24 h, and different concentrations of tested drugs were added into each well. After incubation in the dark for 4 h, the light groups were exposed to LED irradiation (470 nm, 40.5 J/cm^2) for 30 min, and then incubated for another 20 h. The dark control groups were incubated in the dark for 20.5 h. After that, the 200 μL stock MTT solution was added to each well. After 4 h of incubation, the media were removed carefully and DMSO was added into each well. The optical density of each well was measured by a Thermo MK3 Multiscan microplate reader at 570 nm.

Cellular uptake, distribution and uptake mechanism measured by ICP-MS

A549 cells were pre-cultured in 25 cm^2 culture plates for 24 h, then incubated with ruthenium (II) complex (1 μM) for 4 h in the dark. The cells were collected in PBS. Nuclear, mitochondria and cytosolic fractions were separated using the nuclear/mitochondrial extraction kits according to the manufacturer's instructions. The concentration of Ru was determined by inductively coupled plasma mass spectrometer (ICP-MS Thermo Elemental Co., Ltd.).

For studying the cellular uptake mechanism,[2] A549 cells were treated with **Ru-3** or **Ru-4** (1 μM) under three different conditions: (a) Control: the cells were incubated with the complexes for 2 h at 37 °C; (b) Low temperature: the cells were preincubated at 4 °C for 1 h and incubated with the complexes for 2 h at 37 °C; (c) Metabolic inhibition: the cells were preincubated with CCCP (20 μM) for 1 h and incubated with the tested drug for 2 h at 37 °C. The uptake levels were determined using ICP-MS by measuring the Ru content.

Cell morphological studies

A549 cells were co-cultured with medium containing ruthenium (II) complexes (20 μM) for 4 h in

the dark, then the light groups were irradiated with two-photon light source (840 nm, 1.11 W/cm^2) equipped in the confocal microscopy at different times.

Apoptosis assay and JC-1 staining assay

Annexin V-FITC/PI Apoptosis Detection Kit was used for detecting apoptosis and necrosis.[3] A549 cells were incubated with ruthenium (II) complexes for 4 h, then were irradiated for 30 min (470 nm, 40.5 J/cm^2), and were incubated for another 10 hours. Cells were collected and washed three times with PBS, strained with Annexin V-FITC/PI and were determined on a Beckman Coulter CytoFLEX Flow Cytometer. Similar procedures were used for the JC-1 staining assay.

Picogreen staining assay

A549 cells were incubated with ruthenium (II) complexes for 4 h in 25 cm^2 culture plates, then were irradiated for 30 min (470 nm, 40.5 J/cm^2), and were incubated for another 6 hours. The medium was refreshed with TE buffer containing Picogreen. After 1 h, the cells were washed for three times with PBS and analyzed using confocal microscopy (λ_{ex} = 488 nm, λ_{em} = 500-550 nm).

Intracellular NADH level and ATP level

A549 cells were seeded in 6 well plates. After incubation with ruthenium(II) complexes for 4 h, the light groups were irradiated for 30 min (470 nm, 40.5 J/cm^2) while the dark groups were not. The cells were collected and washed with cold PBS, then cellular NADH levels were measured using Coenzyme Ⅰ NAD(H) Content Assay Kit (Solarbio) according to the manufacturer's instructions. Similar procedures were used for the measurement of intracellular ATP level except for the ATP content detection kit was used.

Fluorescence quantum yield measurements

Fluorescence quantum yields of 2-phenylimidazo[4,5-*f*][1,10]phenanthroline (PIP) derivatives were measured according to a reported method[4]. Quinine sulfate was used as the reference with a fluorescence quantum yield of 0.55 in 0.1 M H_2SO_4 at room temperature. The calculation formula was given as below:

$$\Phi = \Phi_{R\times}\frac{I}{I_{R\times}}\frac{A_R}{A}{}_{\times}\frac{n^2}{{n_R}^2}$$

Where Φ is fluorescence quantum yield, I is the integrated emission intensity, A is the absorbance at excitation wavelength, and n is the refractive index. The subscript of 'R' stands for reference (Φ_R = 0.55, n_R = 1.33).

Two-photon absorption cross section measurement

The two-photo absorption (TPA) cross section was measured using the reported method[5]. The samples were placed in fluorometric quartz cuvettes in $CHCl_3$ at room temperature with Rhodamine B as the reference. The experimental fluorescence excitation and detection conditions were conducted with negligible reabsorption processes. The TPA spectra were determined among 700-900 nm, and the cross section was calculated at each wavelength according to the following formula:

$$\delta_2 = \delta_1 \times \frac{\Phi 1}{\Phi 2} \times \frac{c1}{c2} \times \frac{I2}{I1}$$

Where δ is the TPA cross-section, Φ is the quantum yield, c is the sample concentration, and I is the integrated fluorescence intensity. The subscript '1' stands for the reference, '2' stands for the sample.

Generation of 3D multicellular tumor spheroids (MCSs)

A number of 5000 diluted A549/DDP cells were seeded to 1.5% agarose-coated transparent 96-well plates with 200 μL of culture media. Within 2-3 days, MCSs were formed from the cell suspension. The MCSs were cultivated and maintained at 37 °C in a cell culture incubator at 37 °C with 5% CO_2 atmosphere. The cell solution in the inlet was replaced with fresh cell culture media every two days to maintain the growing of MCSs.[6]

Viability assay on 3D multicellular spheroids (MCSs)

3D MCSs were generated as mentioned above. The MCSs were harvested after 3 days of incubation at 37 °C with 5% CO_2, with a diameter around 600 μm. Ruthenium (II) complexes (20 μM) was added and co-incubated with MCSs for 8 h. The light groups were irradiated for 30 min (800 nm, 1 W/cm^2). All groups were incubated for an additional 24 h. After that, all the MCSs were incubated with Calcein-AM and PI solutions for 30 min and imaged using a confocal fluorescence microscope.

Synthesis and characterization

General procedure A: synthesis of ligands

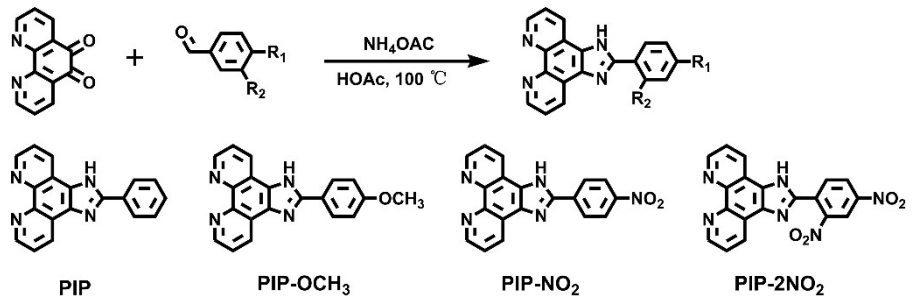

1 mmol of 1,10-phenanthroline-5,6-dione, 1.1 mmol of 2-R_2-4-R_1-benzaldehyde (R_1 = H, OCH_3, NO_2, R_2 = H, NO_2) and 20 mmol of ammonium acetate were added to glacial acetic acid (~15 mL), and the reaction was stirred at 100 ℃ for 3 h. After cooling down to room temperature, 30 mL deionized water was added to the mixture, followed by slow addition of $NH_3 \cdot H_2O$ until pH = 5-6. The resultant precipitate was collected by filtration and washed with water. The crude product was recrystallized from ethanol to yield the pure product.[7-9]

Synthesis and characterization of 2-phenylimidazo[4,5-*f*][1,10]phenanthroline (PIP)[7]

The ligand PIP was prepared according to general procedure A. Yellow solid, yield 58%. ^{1}H NMR (400 MHz, DMSO-d_6) δ 13.76 (s, 1H), 9.04 (d, *J* = 4.0 Hz, 2H), 8.97-8.91 (m, 2H), 8.30 (d, *J* = 7.6 Hz, 2H), 7.85 (ddd, *J* = 17.8, 7.4, 4.0 Hz, 2H), 7.63 (t, *J* = 7.2 Hz, 2H), 7.53 (t, *J* = 7.2 Hz, 1H). HR ESI-MS: PIP, $[M+H]^+$ Calculated: 297.1140, Found: 297.1123.

Synthesis and characterization of 2-(4-methoxyphenyl)imidazo[4,5-*f*][1,10]phenanthroline (PIP-OCH_3)[8]

The ligand PIP-OCH_3 was prepared according to general procedure A. Yellow solid, yield 61%. ^{1}H NMR (400 MHz, DMSO-d_6) δ 13.07 (s, 1H), 9.03 (d, *J* = 7.2 Hz, 2H), 8.92 (d, *J* = 7.2 Hz, 2H), 8.23 (d, *J* = 7.2 Hz, 2H), 7.88-7.78 (m, 2H), 7.19 (d, *J* = 7.2 Hz, 2H), 3.87 (s, 3H). HR ESI-MS: PIP-OCH_3, $[M+H]^+$ Calculated: 327.1246, Found: 327.1235.

Synthesis and characterization of 2-(4-nitrophenyl)imidazo[4,5-*f*][1,10]phenanthroline (PIP-NO_2)[8]

The ligand PIP-NO_2 was prepared according to general procedure A. Yellow solid, yield 73%. ^{1}H NMR (400 MHz, DMSO-d_6) δ 14.11 (s, 1H), 9.06 (t, *J* = 4.3 Hz, 2H), 8.93 (dd, *J* = 6.9, 3.9 Hz, 2H), 8.52 (dd, *J* = 15.2, 8.9 Hz, 4H), 7.86 (m, 2H). HR ESI-MS: PIP-NO_2, $[M+H]^+$ Calculated: 342.0991, Found: 342.0979.

Synthesis and characterization of 2-(2,4-dinitrophenyl)imidazo[4,5-*f*][1,10]phenanthroline (PIP-$2NO_2$)[9]

The ligand PIP-$2NO_2$ was prepared according to general procedure A. Yellow solid, yield 69%. ^{1}H NMR (400 MHz, DMSO-d_6) δ 14.40 (s, 1H), 9.08 (d, *J* = 4.1 Hz, 2H), 8.91 (d, *J* = 2.6 Hz, 1H), 8.86-8.72 (m, 3H), 8.44 (d, *J* = 8.6 Hz, 1H), 7.87 (s, 2H). HR ESI-MS: PIP-$2NO_2$, $[M+H]^+$ Calculated: 387.0842, Found: 387.0872.

General procedure B: synthesis of ruthenium (II) complexes

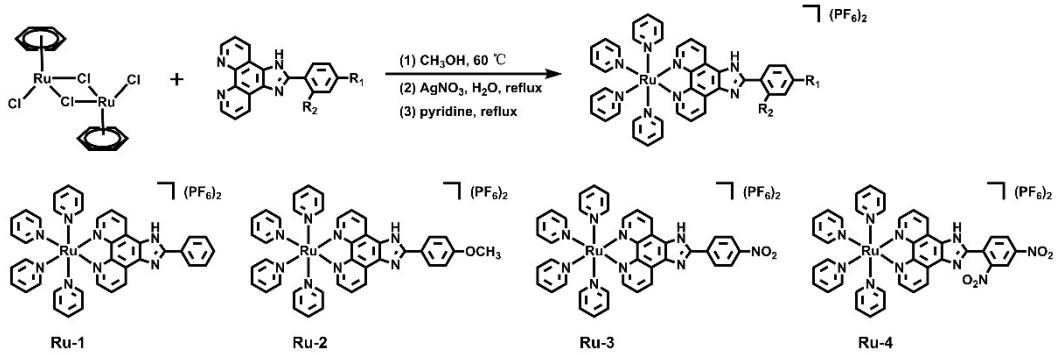

A mixture of 0.6 mmol of dichloro(benzene) ruthenium (II) dimer and 1.2 mmol of ligand was suspended in 30 mL methanol and was heated at 60 °C for 4 h under an argon atmosphere. Then 3 mmol of $AgNO_3$ in aqueous solution (10 mL) was added, and the mixture was refluxed for 4 h. After that, 10 mL pyridine was added, and the solution was refluxed for another 4 h. After cooling to room temperature, the solvent was evaporated under reduced pressure and the crude product was purified by column chromatography on silica gel using CH_3CN/H_2O (KNO_3) = 10 : 1 as the eluent. The pure compound was dissolved in water, and saturated NH_4PF_6 aqueous solution was added. The resultant red precipitate was collected by filtration and dried under vacuum.

Synthesis and characterization of $[Ru(py)_4(PIP)](PF_6)_2$ (Ru-1)

Ru-1 was prepared according to general procedure B. Red solid, yield 53%. ^{1}H NMR (400 MHz, CD_3CN) δ 9.05 (d, *J* = 8.3 Hz, 2H), 8.84 (d, *J* = 5.4 Hz, 2H), 8.43 (d, *J* = 5.7 Hz, 4H), 8.29 (d, *J* = 7.5 Hz, 2H), 8.09 (t, *J* = 7.8 Hz, 2H), 8.00 (dd, *J* = 8.3, 5.5 Hz, 2H), 7.76-7.54 (m, 13H), 7.05 (t, *J* = 6.9 Hz, 4H). HR ESI-MS: **Ru-1**, $[M-2PF_6^-]^{2+}$ Calculated: 357.0891, Found: 357.0888. HPLC purity > 95%.

Synthesis and characterization of $[Ru(py)_4(PIP\text{-}OCH_3)](PF_6)_2$ (Ru-2)

Ru-2 was prepared according to general procedure B. Red solid, yield 68%. ^{1}H NMR (400 MHz, CD_3CN) δ 9.05 (s, 2H), 8.80 (d, *J* = 5.3 Hz, 2H), 8.42 (d, *J* = 5.6 Hz, 4H), 8.24 (d, *J* = 8.4 Hz, 2H), 8.08 (t, *J* = 7.7 Hz, 2H), 7.97 (dd, *J* = 8.2, 5.4 Hz, 2H), 7.71 (t, *J* = 6.4 Hz, 6H), 7.56 (t, *J* = 6.6 Hz,

4H), 7.17 (d, J = 8.4 Hz, 2H), 7.04 (t, J = 6.7 Hz, 4H), 3.91 (s, 3H). HR ESI-MS: **Ru-2**, $[M\text{-}2PF_6^-]^{2+}$ Calculated: 372.0944, Found: 372.0939. HPLC purity > 95%.

Synthesis and characterization of $[Ru(py)_4(PIP\text{-}NO_2)](PF_6)_2$ (Ru-3)

Ru-3 was prepared according to general procedure B. Red solid, yield 49%. ^{1}H NMR (400 MHz, CD_3CN) δ 9.04 (d, J = 8.0 Hz, 2H), 8.85 (d, J = 5.4 Hz, 2H), 8.48 (dd, J = 11.3, 9.2 Hz, 4H), 8.42 (d, J = 5.4 Hz, 4H), 8.09 (t, J = 7.6 Hz, 2H), 8.01 (dd, J = 8.2, 5.4 Hz, 2H), 7.76-7.66 (m, 6H), 7.57 (t, J = 6.9 Hz, 4H), 7.05 (dd, J = 8.2, 5.7 Hz, 4H). HR ESI-MS: **Ru-3**, $[M\text{-}2PF_6^-]^{2+}$ Calculated: 379.5817, Found: 379.5813. HPLC purity > 95%.

Synthesis and characterization of $[Ru(py)_4(PIP\text{-}2NO_2)](PF_6)_2$ (Ru-4)

Ru-4 was prepared according to general procedure B. Red solid, yield 63%. ^{1}H NMR (400 MHz, CD_3CN) δ 9.01 (d, J = 8.2 Hz, 2H), 8.72 (d, J = 5.2 Hz, 2H), 8.57 (d, J = 8.5 Hz, 2H), 8.50 (dd, J = 8.7, 2.0 Hz, 1H), 8.44 (d, J = 5.4 Hz, 4H), 8.07 (t, J = 7.6 Hz, 2H), 7.89 (dd, J = 8.1, 5.4 Hz, 2H), 7.75-7.65 (m, 6H), 7.55 (t, J = 6.9 Hz, 4H), 7.04 (t, J = 6.9 Hz, 4H). HR ESI-MS: **Ru-4**, $[M\text{-}2PF_6^-]^{2+}$ Calculated: 402.0742, Found: 402.0736. HPLC purity > 95%.

Supporting Tables and Figures

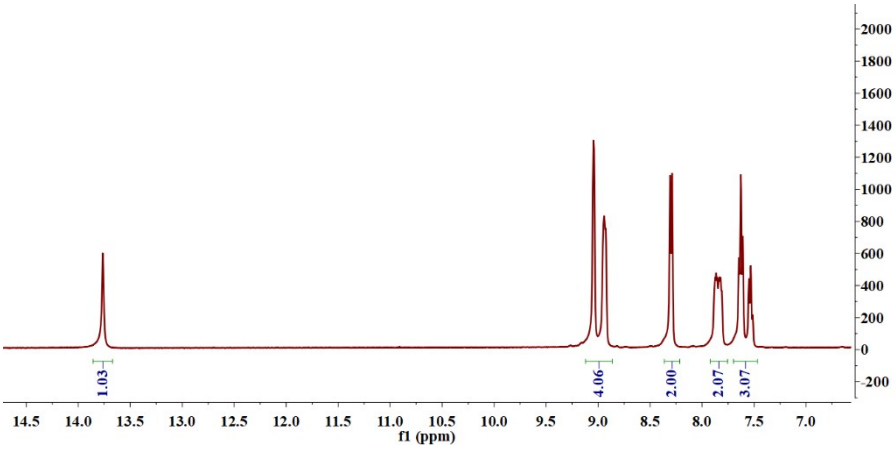

Fig. S1 ^{1}H NMR spectrum of **PIP** in DMSO-d_6.

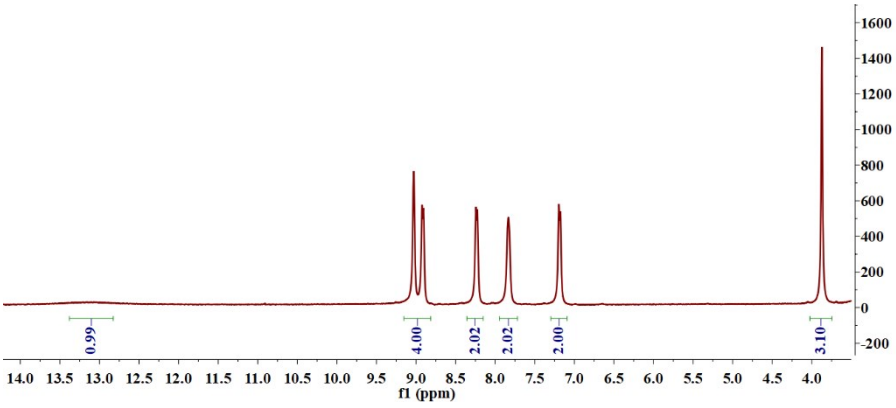

Fig. S2 ^{1}H NMR spectrum of **PIP-OCH$_3$** in DMSO-d_6.

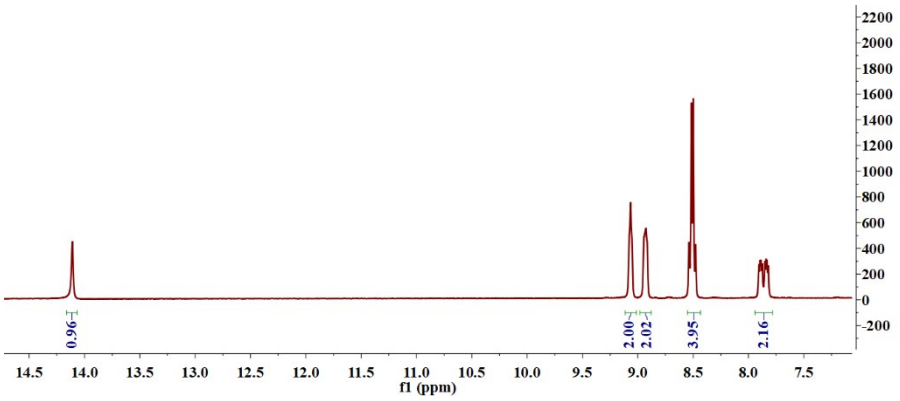

Fig. S3 ^{1}H NMR spectrum of **PIP-NO$_2$** in DMSO-d$_6$.

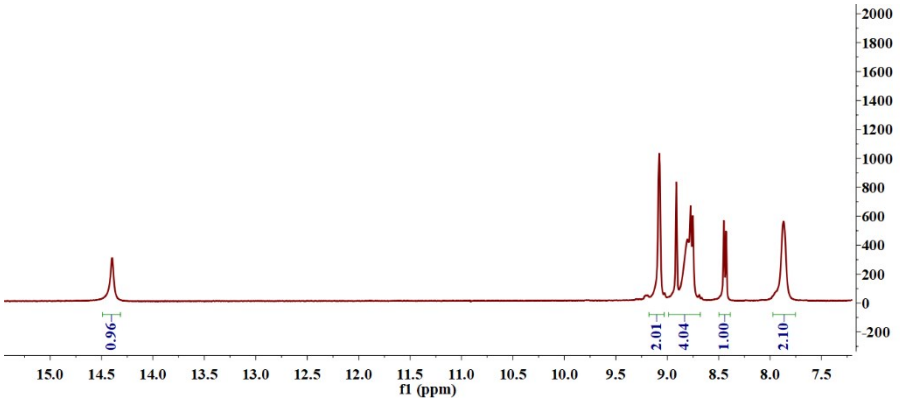

Fig. S4 ^{1}H NMR spectrum of **PIP-2NO$_2$** in DMSO-d$_6$.

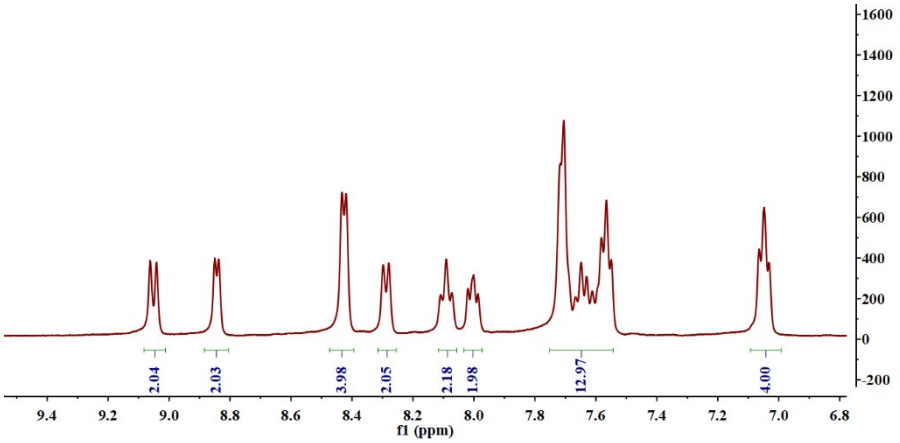

Fig. S5 ^{1}H NMR spectrum of **Ru-1** in CD$_3$CN.

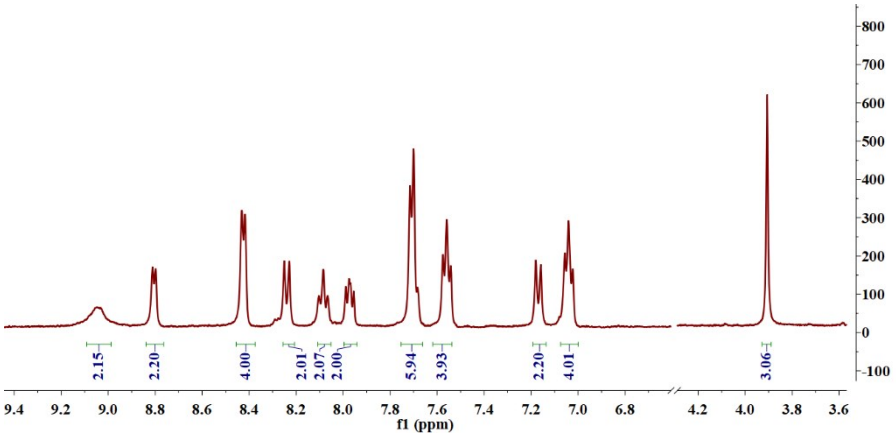

Fig. S6 ^{1}H NMR spectrum of **Ru-2** in CD_3CN.

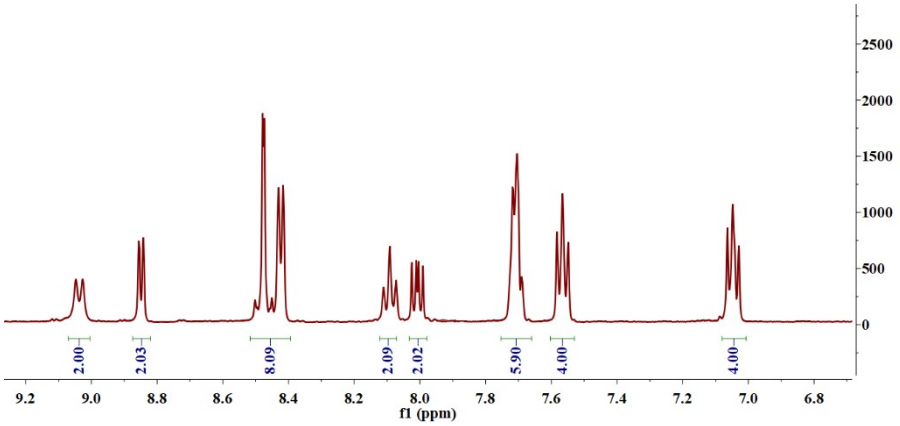

Fig. S7 ^{1}H NMR spectrum of **Ru-3** in CD_3CN.

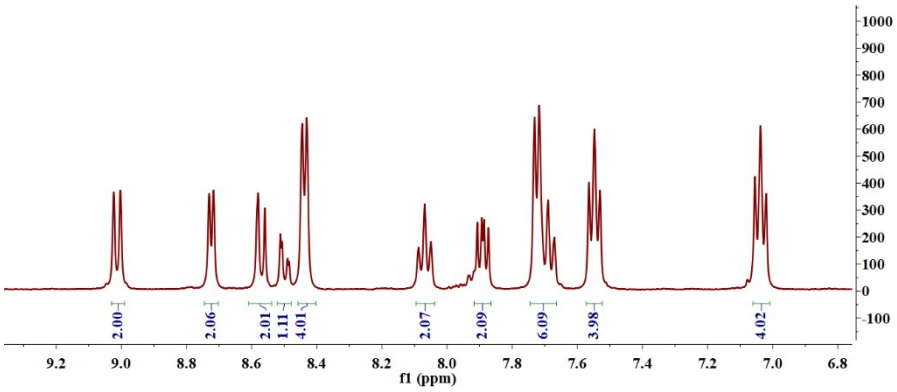

Fig. S8 ^{1}H NMR spectrum of **Ru-4** in CD_3CN.

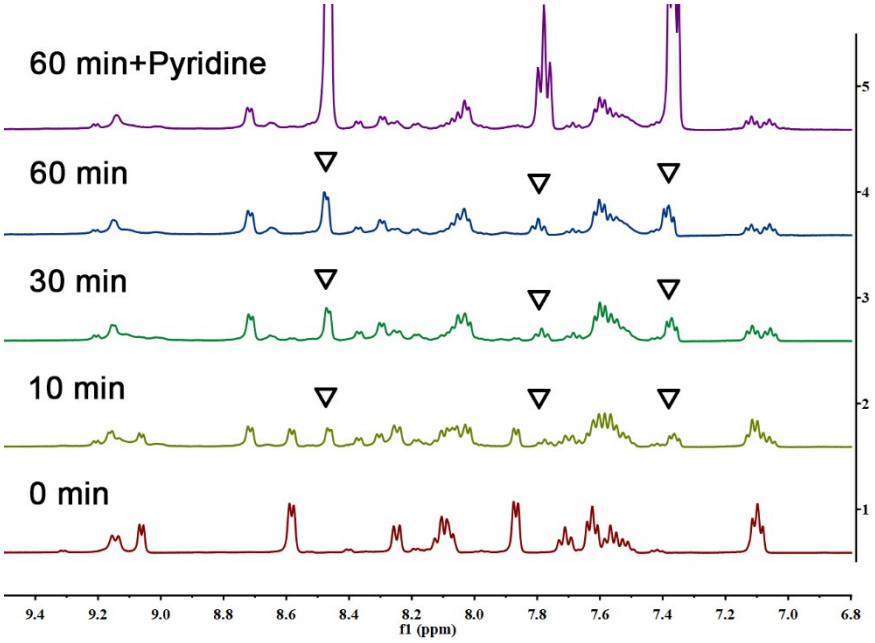

Fig. S9 ^{1}H NMR spectral changes of **Ru-1** upon irradiation with different times (470 nm, 40.5 J/cm^2) in CD_3COCD_3/D_2O (2 : 1).▽ represents the free pyridine based signals.

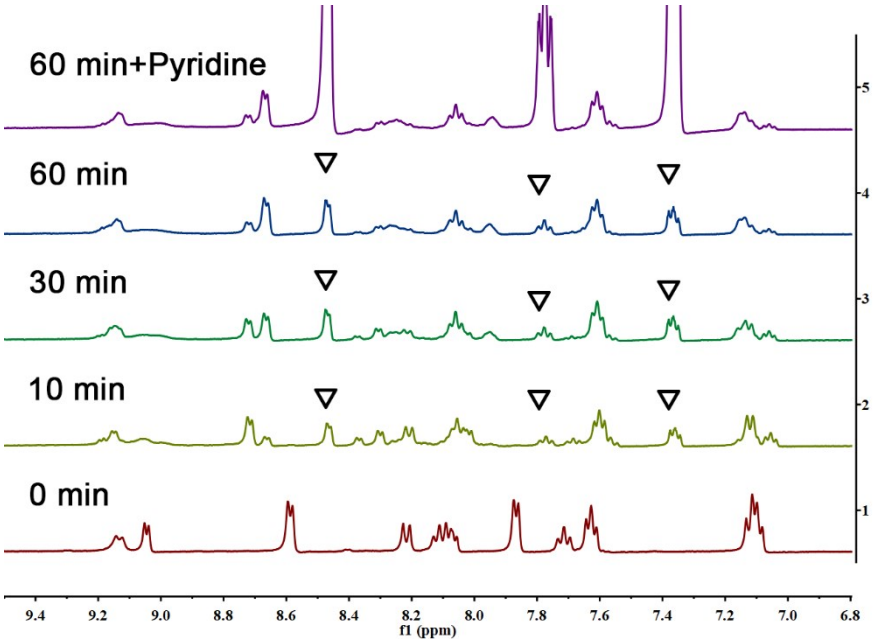

Fig. S10 ^{1}H NMR spectral changes of **Ru-2** upon irradiation with different times (470 nm, 40.5 J/cm^2) in CD_3COCD_3/D_2O (2 : 1). ▽ represents the free pyridine based signals.

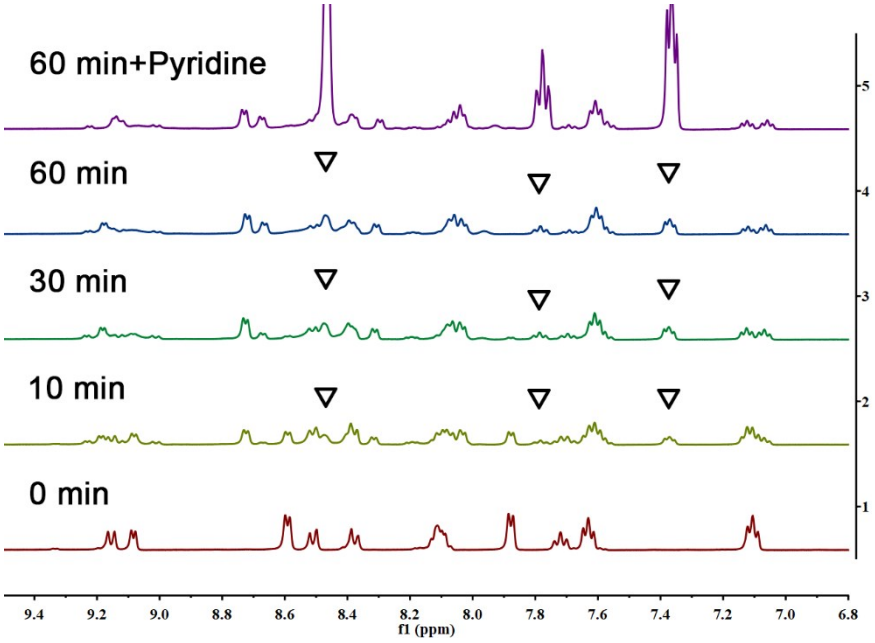

Fig. S11 ^{1}H NMR spectral changes of **Ru-3** upon irradiation with different times (470 nm, 40.5 J/cm^2) in CD_3COCD_3/D_2O (2 : 1). ▽ represents the free pyridine based signals.

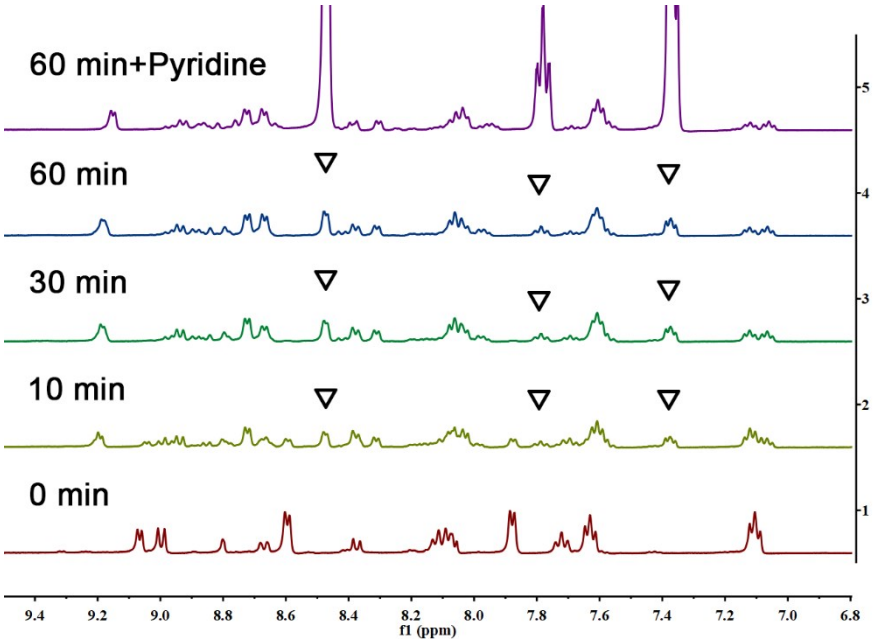

Fig. S12 ^{1}H NMR spectral changes of **Ru-4** upon irradiation with different times (470 nm, 40.5 J/cm^2) in CD_3COCD_3/D_2O (2 : 1). ▽ represents the free pyridine based signals.

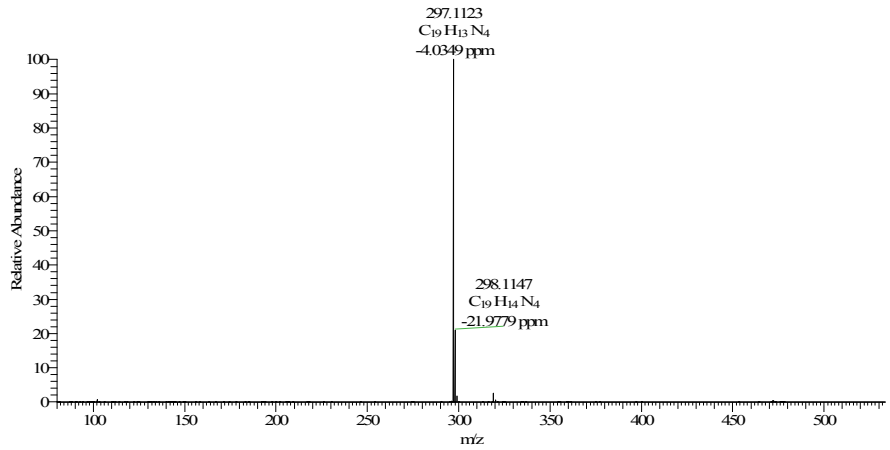

Fig. S13 ESI-MS spectrum of **PIP** ligand.

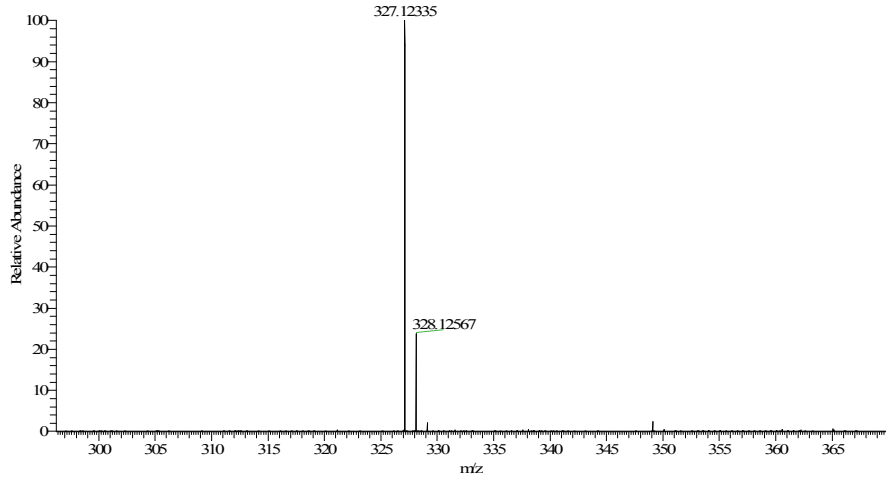

Fig. S14 ESI-MS spectrum of **PIP-OCH_3** ligand.

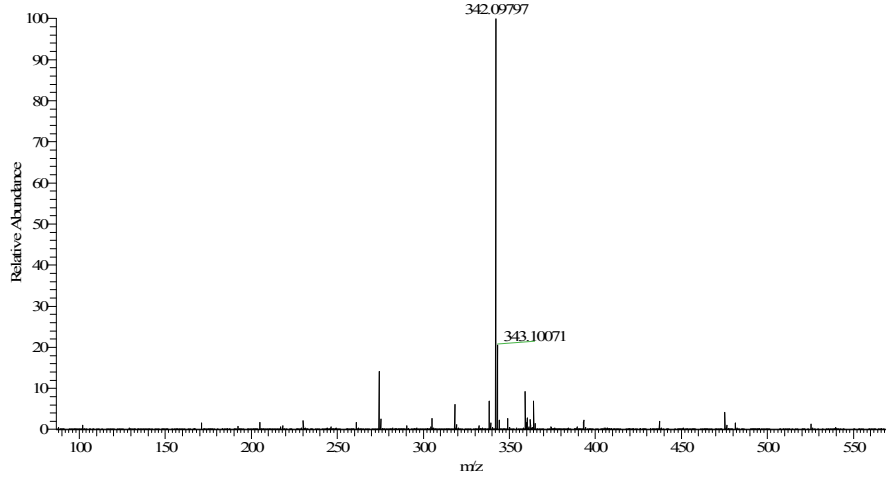

Fig. S15 ESI-MS spectrum of **PIP-NO_2** ligand.

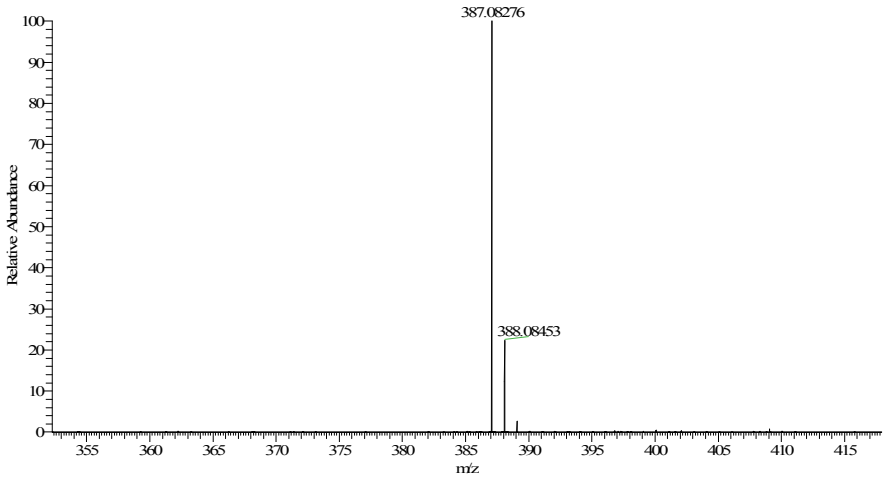

Fig. S16 ESI-MS spectrum of **PIP-2NO$_2$** ligand.

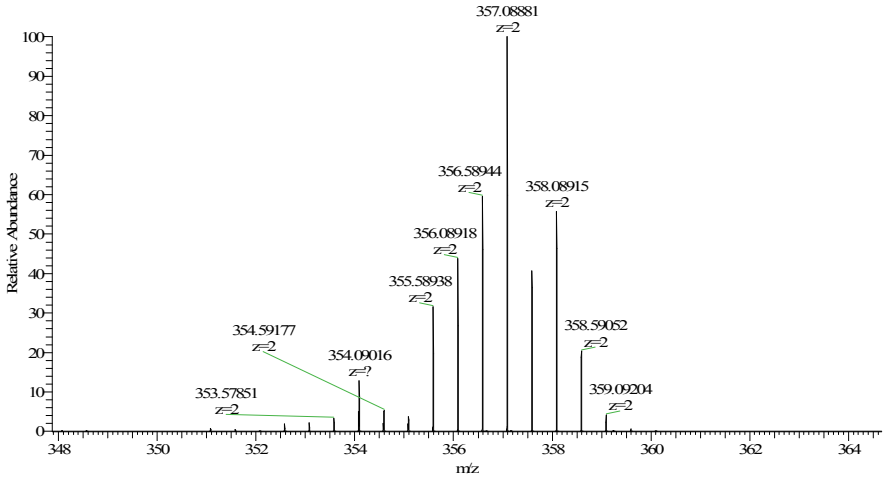

Fig. S17 ESI-MS spectrum of **Ru-1**.

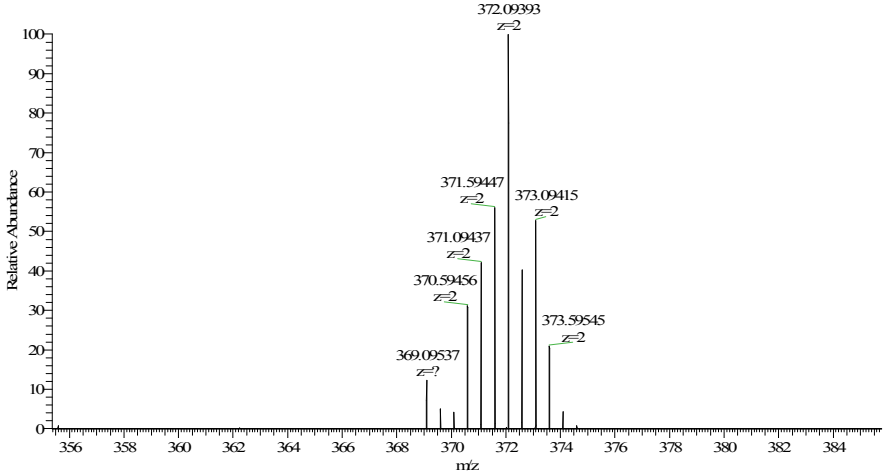

Fig. S18 ESI-MS spectrum of **Ru-2**.

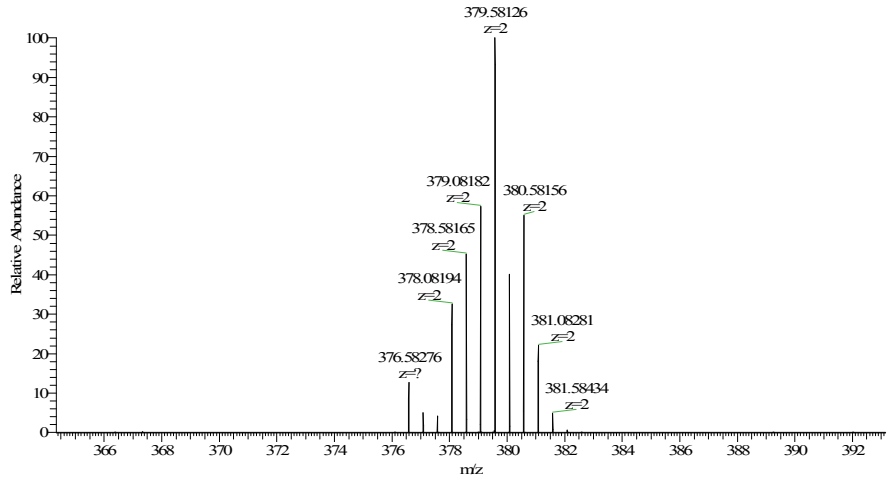

Fig. S19 ESI-MS spectrum of **Ru-3**.

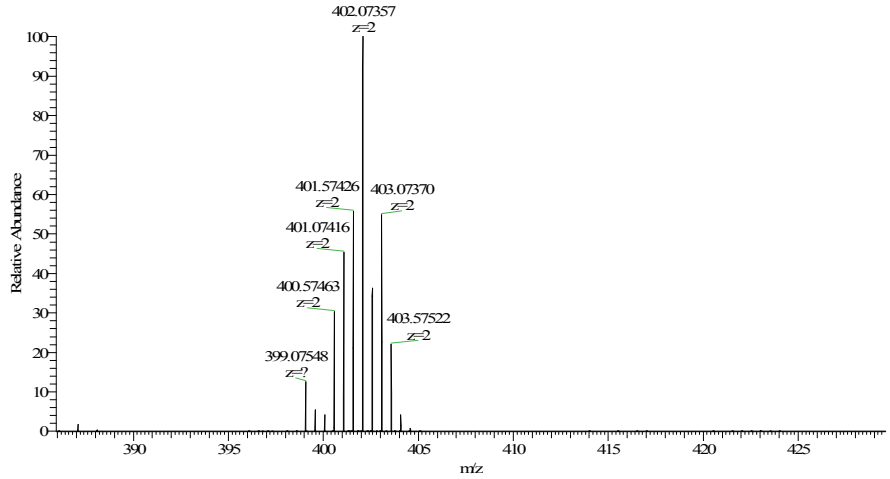

Fig. S20 ESI-MS spectrum of **Ru-4**.

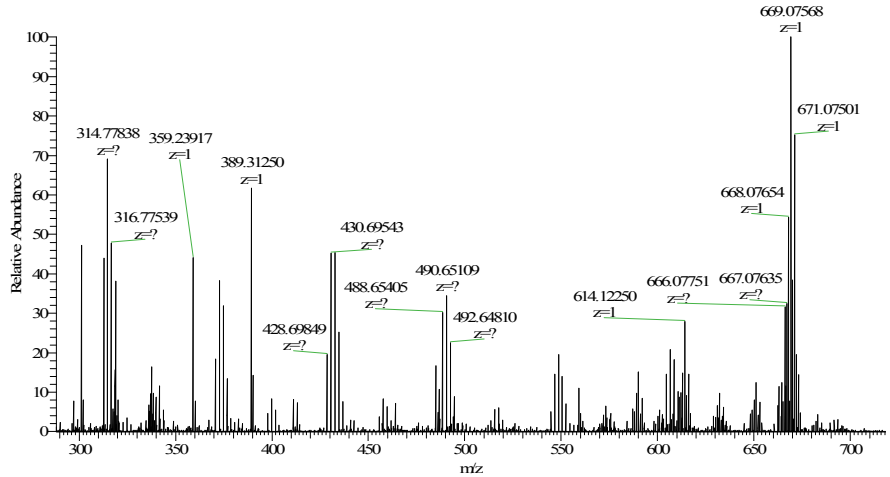

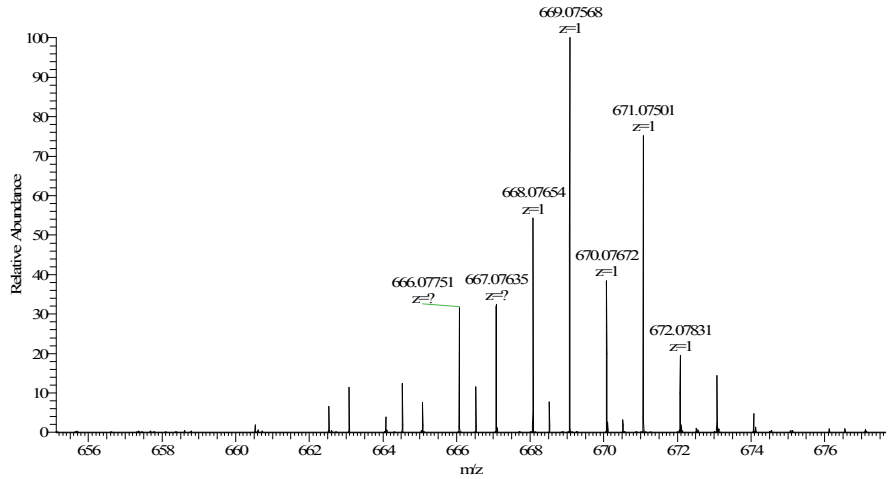

Fig. S21 ESI-MS spectra of **Ru-1** after one-photon irradiation (470 nm, 40.5 J/cm^2, 30 min) in PBS (containing 0.1% DMSO). The m/z peak at 669.0757 can be ascribed to $[Ru(py)_2(PIP)(DMSO)(Cl)]^+$. HR ESI-MS: $[Ru(py)_2(PIP)(DMSO)(Cl)]^+$ calculated: 669.0777, Found: 669.0757.

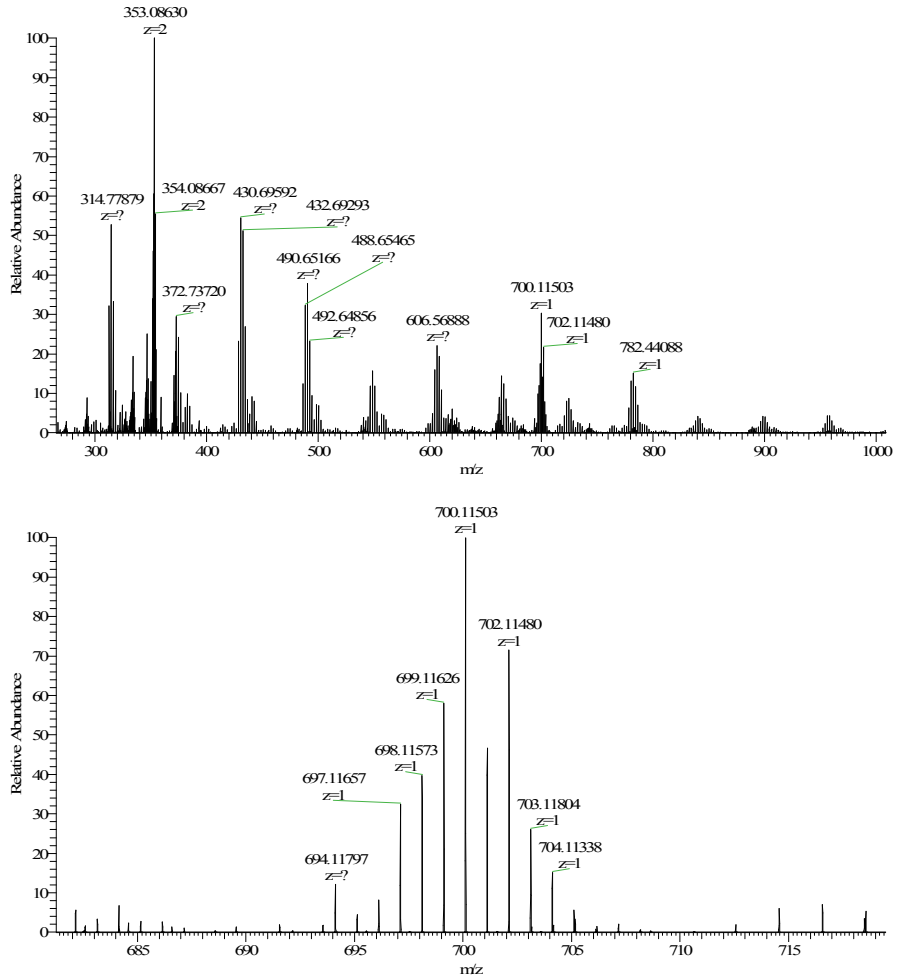

Fig. S22 ESI-MS spectra of **Ru-2** after one-photon irradiation (470 nm, 40.5 J/cm^2, 30 min) in PBS (containing 0.1% DMSO). The m/z peak at 700.1150 can be ascribed to $[Ru(py)_3(PIP\text{-}OCH_3)(Cl)]^+$. HR ESI-MS: $[Ru(py)_3(PIP\text{-}OCH_3)(Cl)]^+$ calculated: 700.1166, Found: 700.1150.

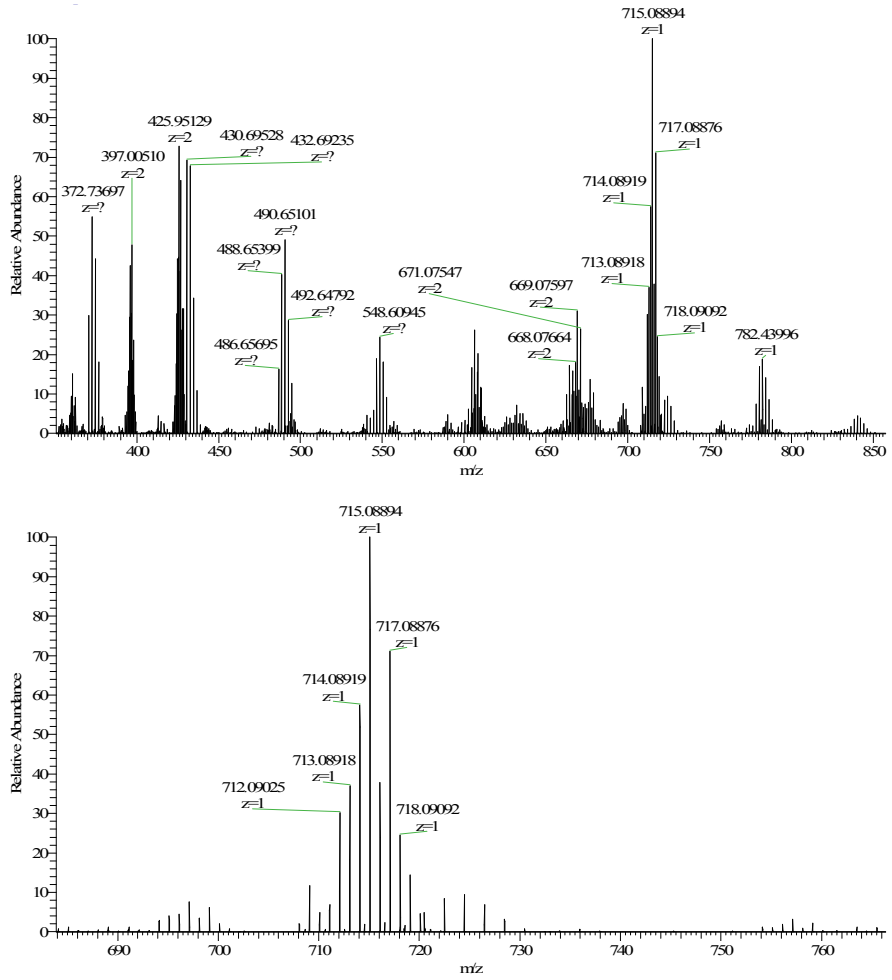

Fig. S23 ESI-MS spectra of **Ru-3** after one-photon irradiation (470 nm, 40.5 J/cm^2, 30 min) in PBS (containing 0.1% DMSO). The m/z peak at 715.0889 can be ascribed to $[Ru(py)_3(PIP\text{-}NO_2)(Cl)]^+$. HR ESI-MS: $[Ru(py)_3(PIP\text{-}NO_2)(Cl)]^+$ calculated: 715.0911, Found: 715.0889.

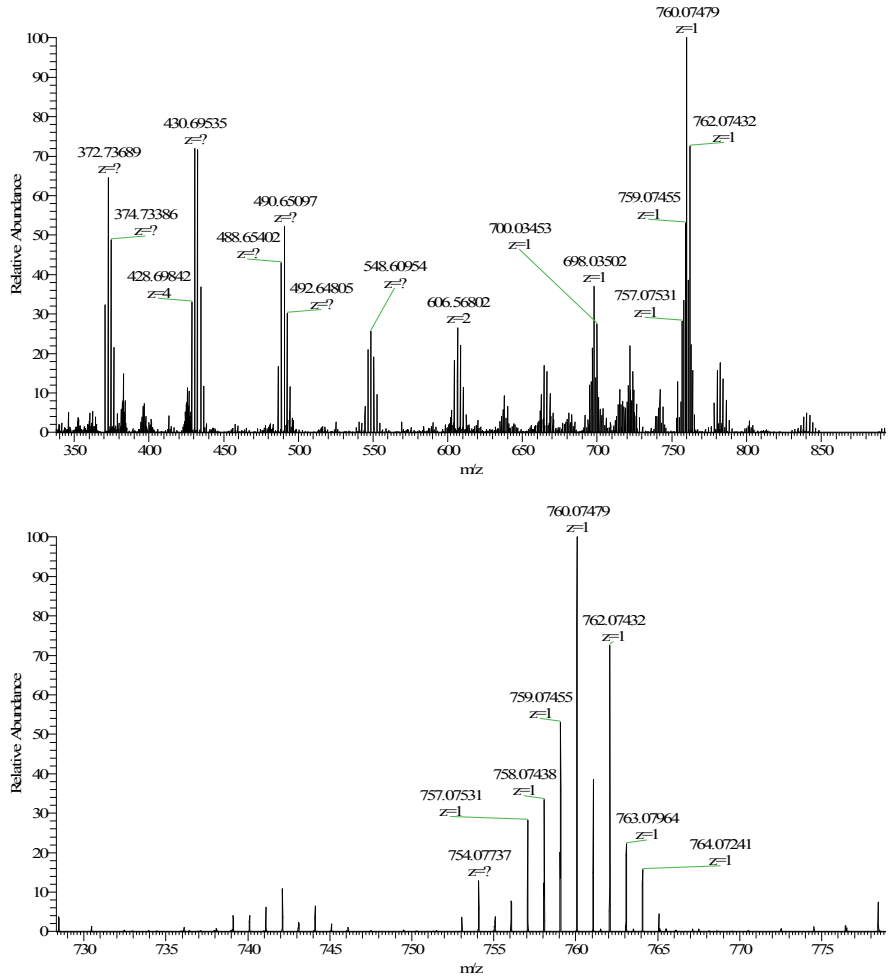

Fig. S24 ESI-MS spectra of **Ru-4** after one-photon irradiation (470 nm, 40.5 J/cm^2, 30 min) in PBS (containing 0.1% DMSO). The m/z peak at 760.0748 can be ascribed to $[Ru(py)_3(PIP\text{-}2NO_2)(Cl)]^+$. HR ESI-MS: $[Ru(py)_3(PIP\text{-}2NO_2)(Cl)]^+$ calculated: 760.0762, Found: 760.0748.

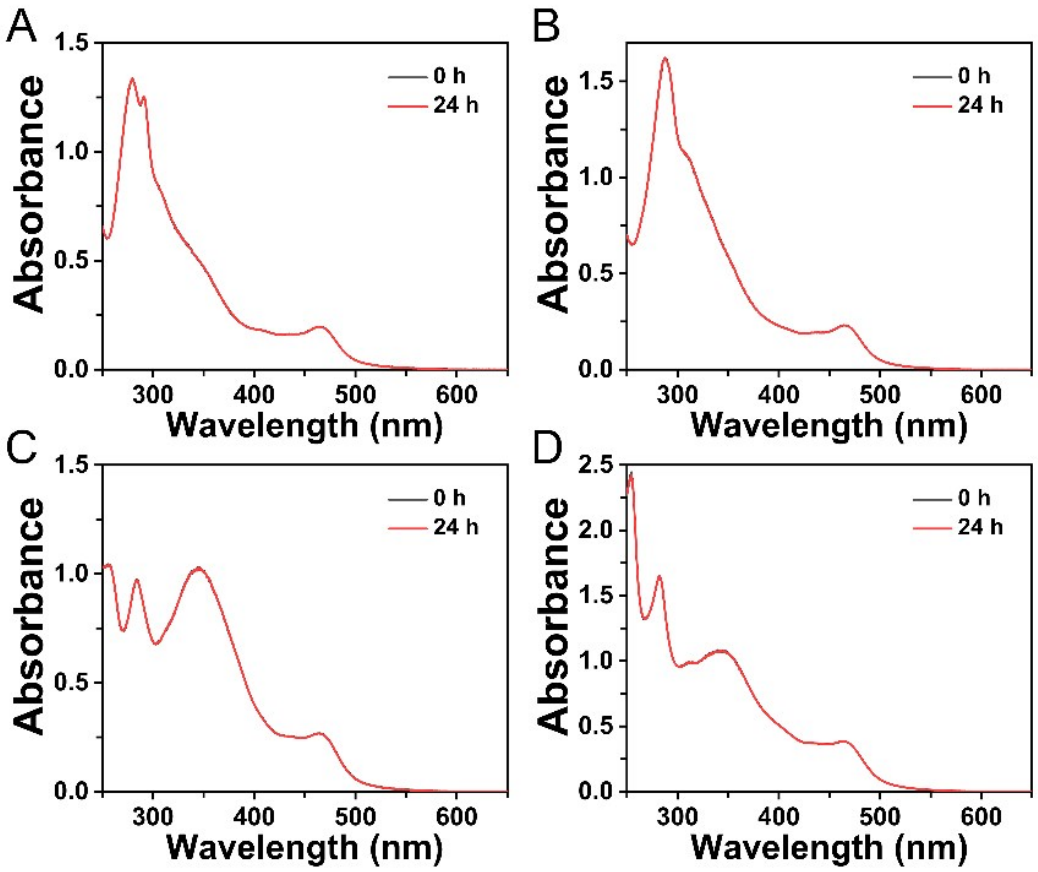

Fig. S25 Absorption spectra changes of **Ru-1** (A), **Ru-2** (B), **Ru-3** (C) and **Ru-4** (D) in H_2O in the dark.

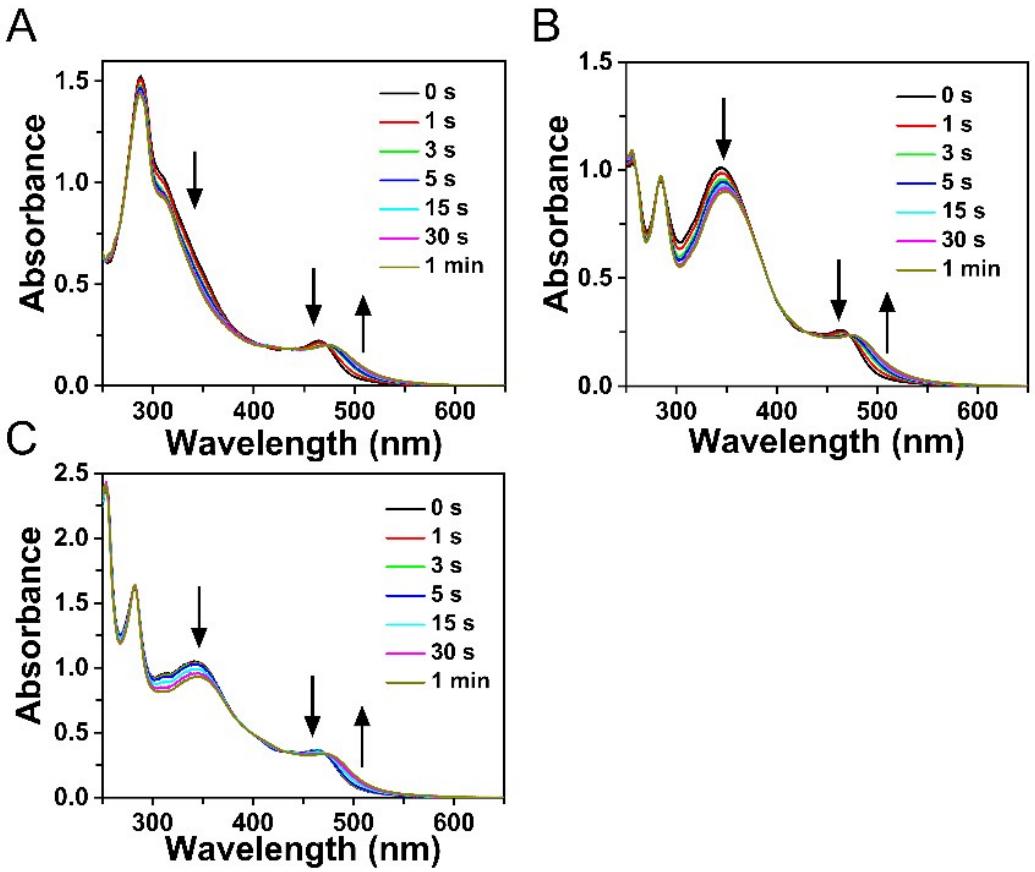

Fig. S26 Absorption spectra changes of **Ru-2** (A), **Ru-3** (B) and **Ru-4** (C) in H_2O upon one-photon irradiation (470 nm, 40.5 J/cm^2).

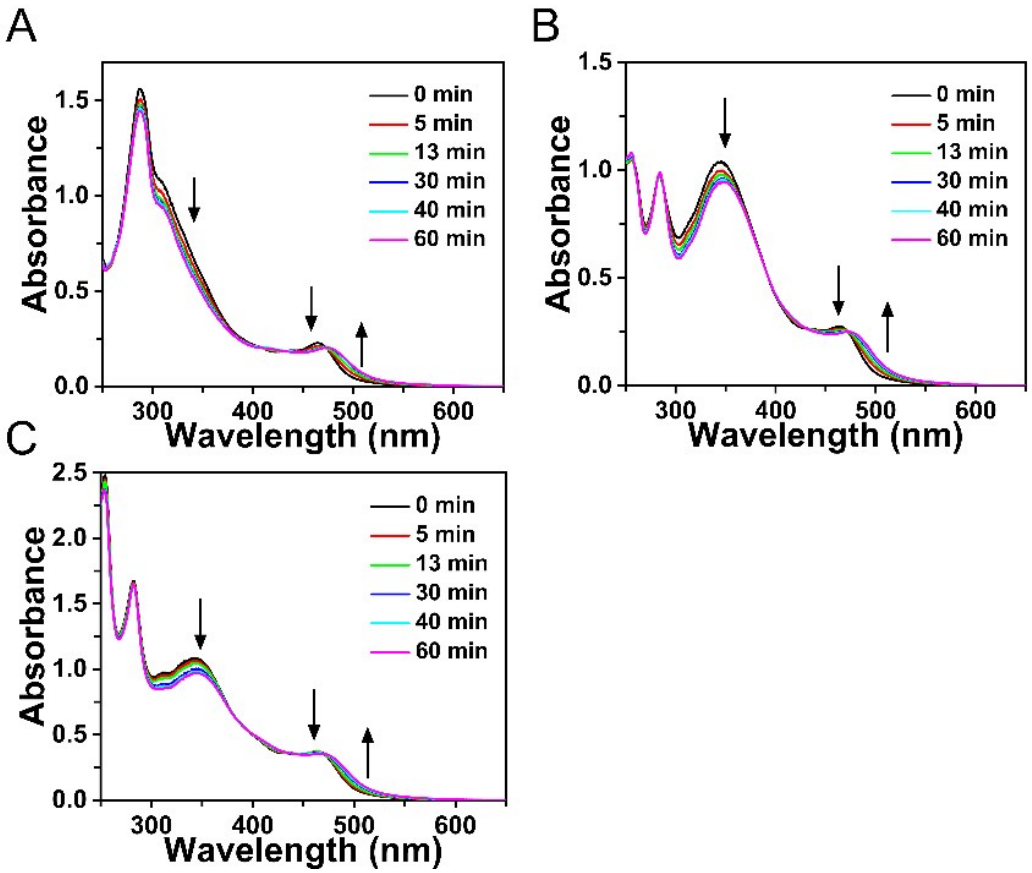

Fig. S27 Absorption spectra changes of **Ru-2** (A), **Ru-3** (B) and **Ru-4** (C) in H_2O upon two-photon irradiation (800 nm, 1 W/cm^2).

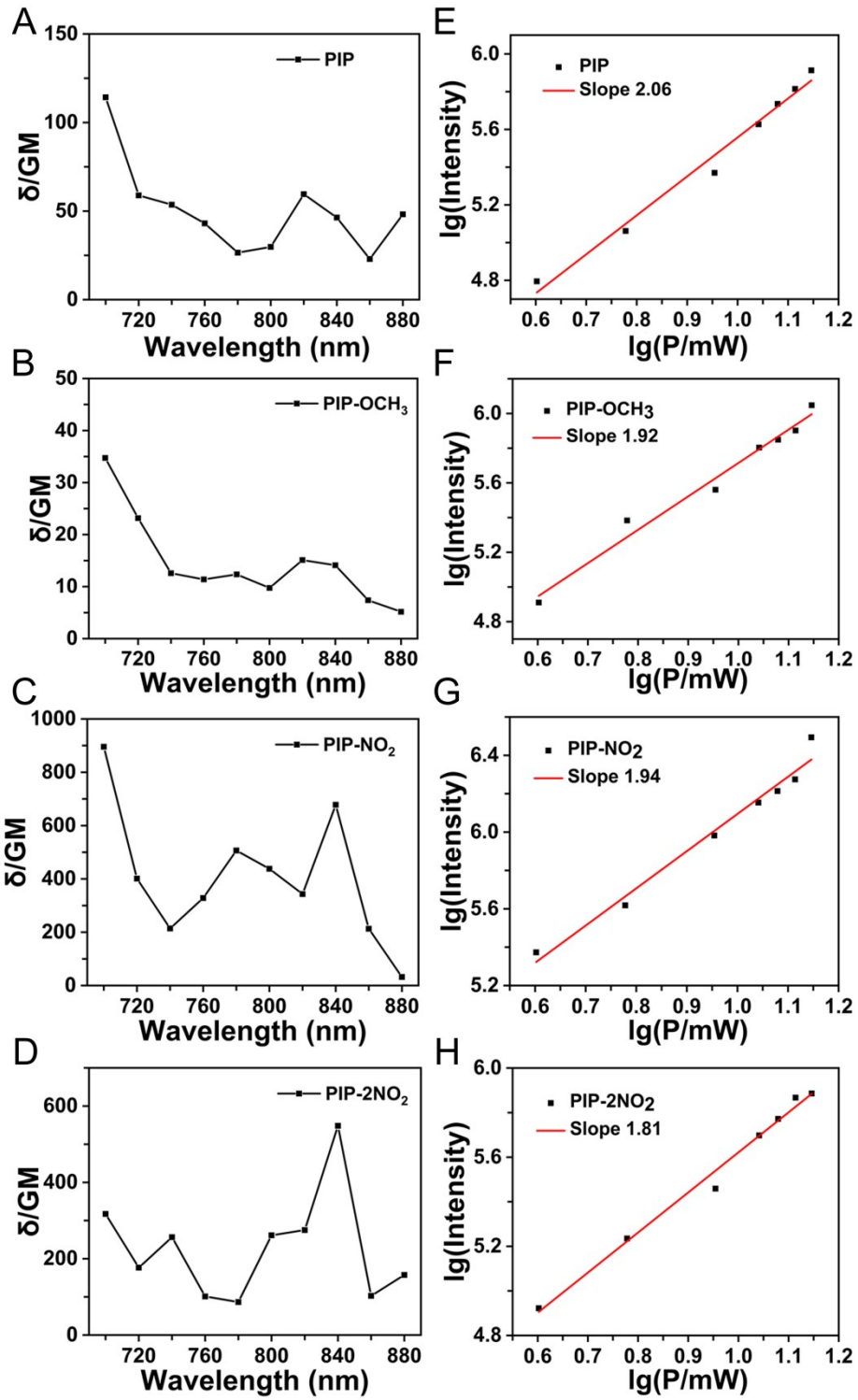

Fig. S28 Two-photon absorption cross sections of ligand **PIP** (A), **PIP-OCH$_3$** (B), **PIP-NO$_2$** (C) and **PIP-2NO$_2$** (D) at different excitation wavelengths from 700 to 880 nm in $CHCl_3$. E-H: The logarithmic plots of the power dependence of relative two-photon induced luminescence intensity as a function of pump power at an excitation wavelength of 740 nm.

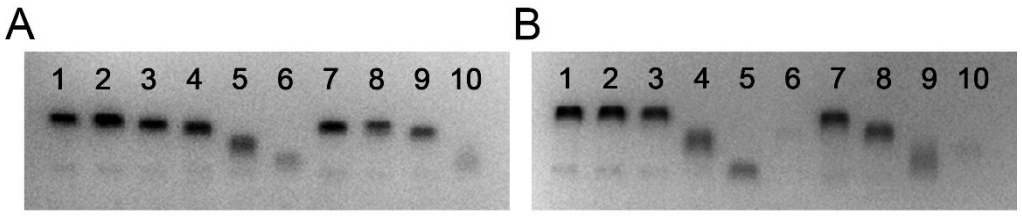

Fig. S29 Agarose gel electrophoresis pattern of pBR322 DNA in air-saturated Tris-CH_3COOH/ EDTA buffer (pH = 8.0) in the presence of **Ru-1** and **Ru-2** (A), and **Ru-3** and **Ru-4** (B) with varied concentrations in the dark or upon irradiation (470 nm, 27 J/cm^2 ,20 min). (A) Lane 1: DNA + dark; Lane 2: DNA + light; Lane 3: **Ru-1** + dark (200 μM); Lane 4-6: **Ru-1** + light with concentrations of 1, 2 and 3 μM, respecively; Lane 7: **Ru-2** + dark (200 μM); Lane 8-10: **Ru-2** + light with concentrations of 1, 2 and 3 μM, respectively. (B) Lane 1: DNA + dark; Lane 2: DNA + light; Lane 3: **Ru-3** + dark (200 μM); Lane 4-6: **Ru-3** + light with concentrations of 0.5, 1 and 2 μM, respectively; Lane 7: **Ru-4** + dark (200 μM); Lane 8-10: **Ru-4** + light with concentrations of 0.5, 1 and 2 μM, respectively.

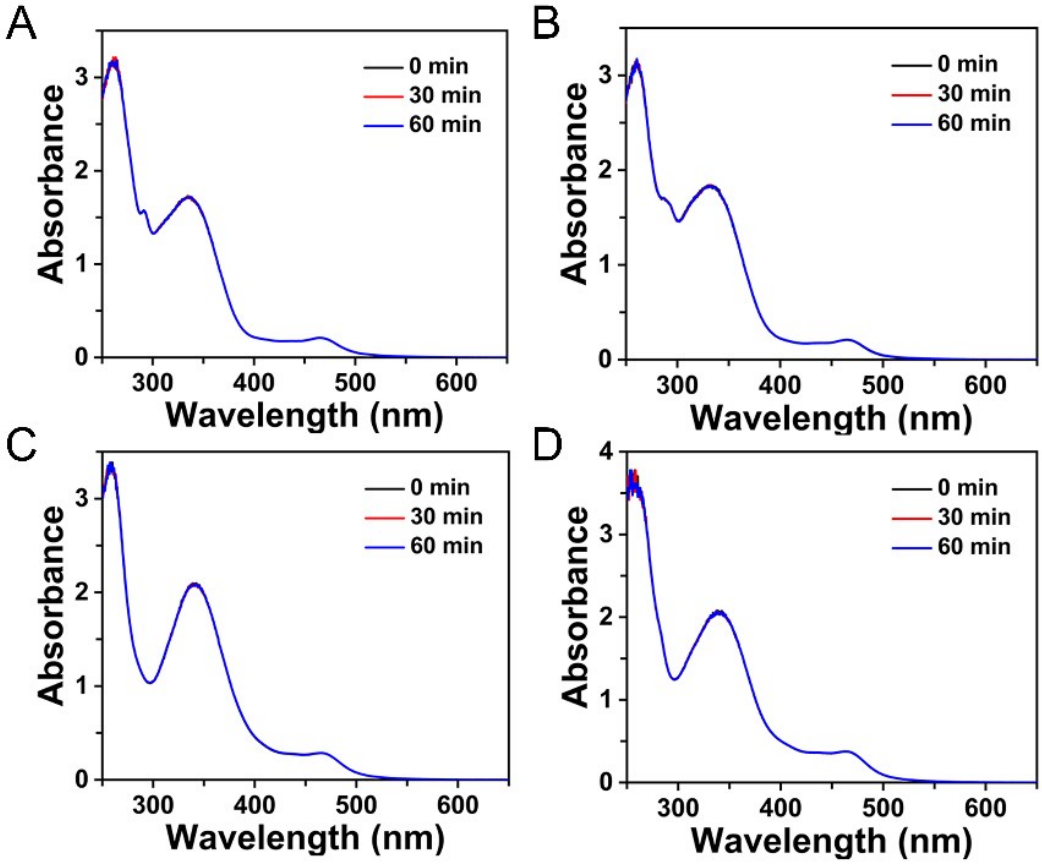

Fig. S30 Absorption spectra changes of NADH (200 μM) in the presence of **Ru-1** (A), **Ru-2** (B), **Ru-3** (C) or **Ru-4** (D) (20 μM) in H_2O in the dark.

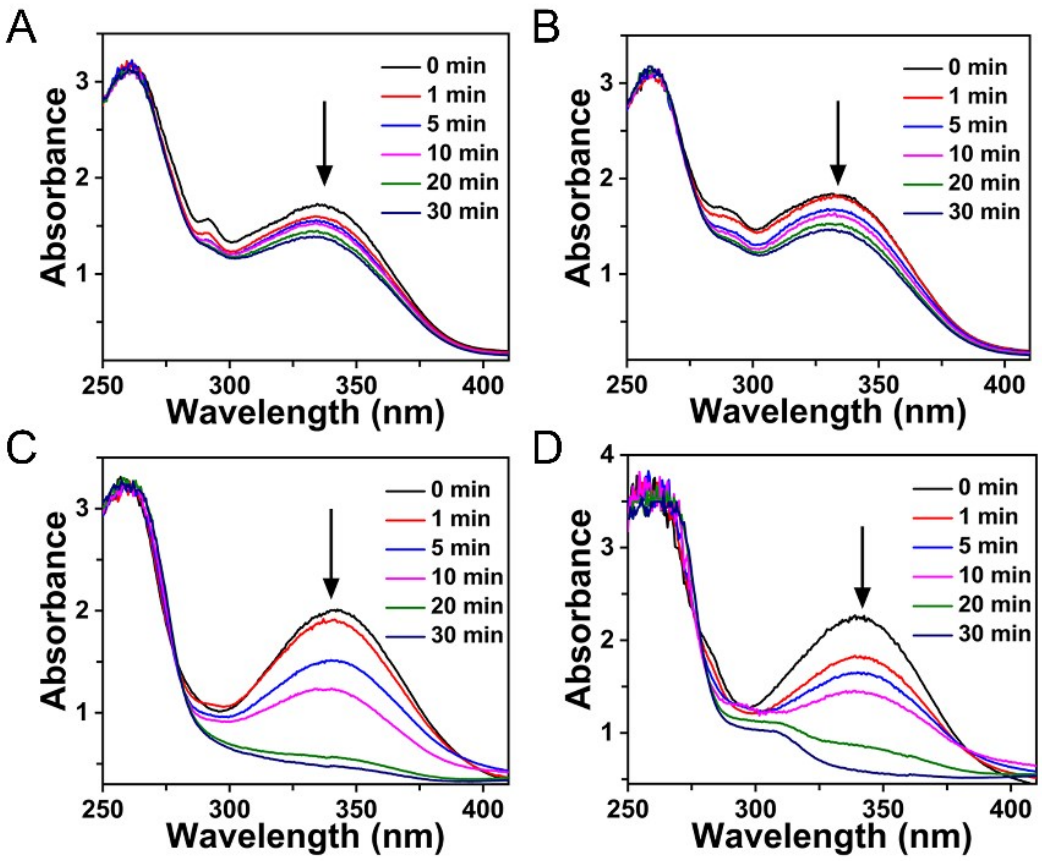

Fig. S31 Absorption spectra changes of NADH (200 μM) in the presence of **Ru-1** (A), **Ru-2** (B), **Ru-3** (C) or **Ru-4** (D) (20 μM) in H_2O upon irradiation (470 nm, 40.5 J/cm^2).

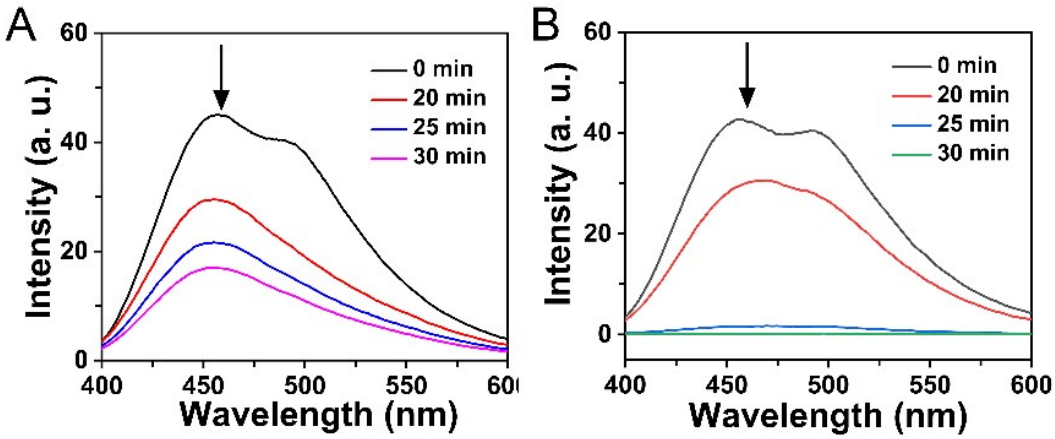

Fig. S32 Emission spectra changes of **NADH** (200 μM) in the present of **Ru-3** (A) or **Ru-4** (B) (20 μM) in H_2O upon LED irradiation (470 nm, 40.5 J/cm^2).

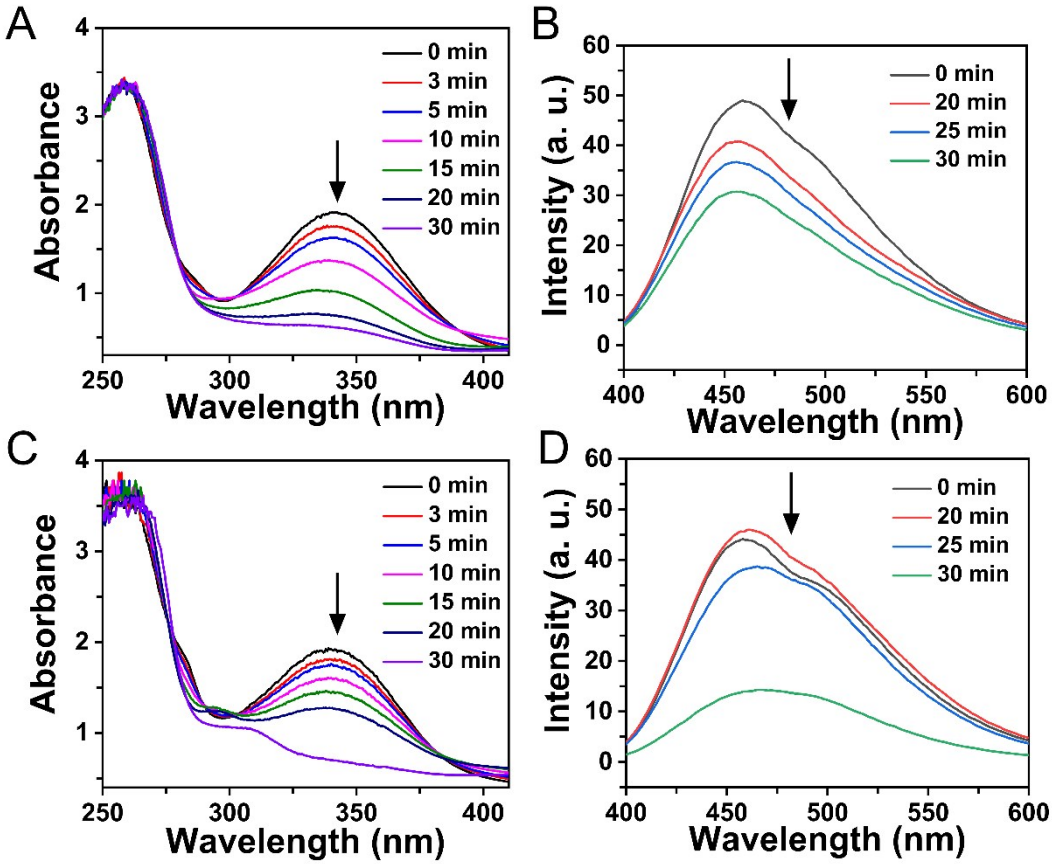

Fig. S33 Absorption (A, C) and emission (B, D) spectra changes of NADH (200 μM) in the presence of the photo-products (**Ru-3** or **Ru-4** were pre-irradiated for 10 min) of **Ru-3** (A, B) or **Ru-4** (C, D) (20 μM) upon irradiation (470 nm, 40.5 J/cm^2).

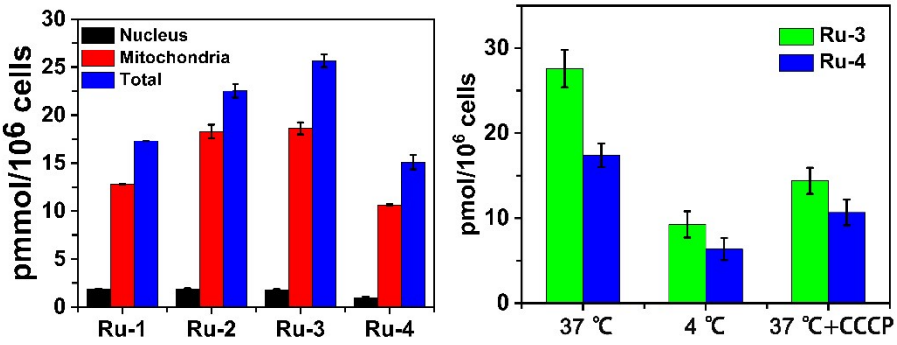

Fig. S34 A549 cellular uptake and subcellular distribution of **Ru-1**-**Ru-4** (1 μM, left), and uptake of **Ru-3** and **Ru-4** under different conditions (1 μM, right), measured by Ru content using ICP-MS.

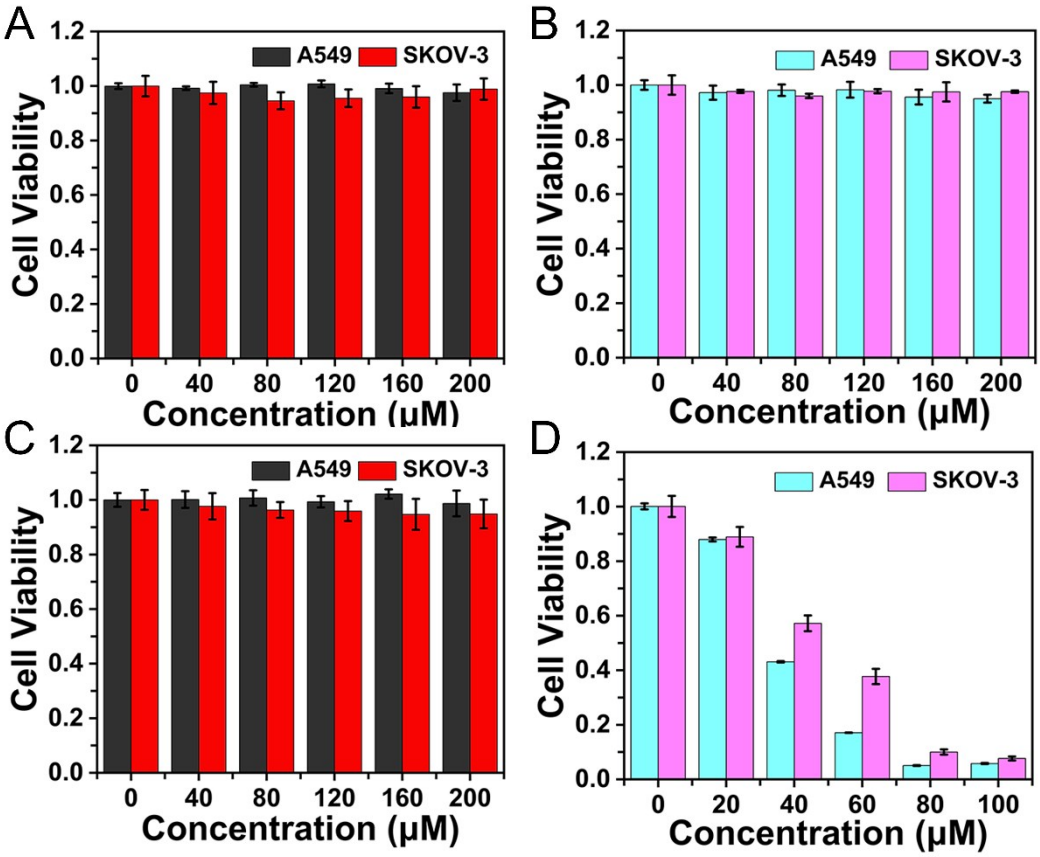

Fig. S35 Cell viability of A549 and SKOV-3 treated with **Ru-1** (A, B) and **Ru-2** (C, D) in the dark (A, C) or upon irradiation (B, D) for 30 min (470 nm, 40.5 J/cm^2).

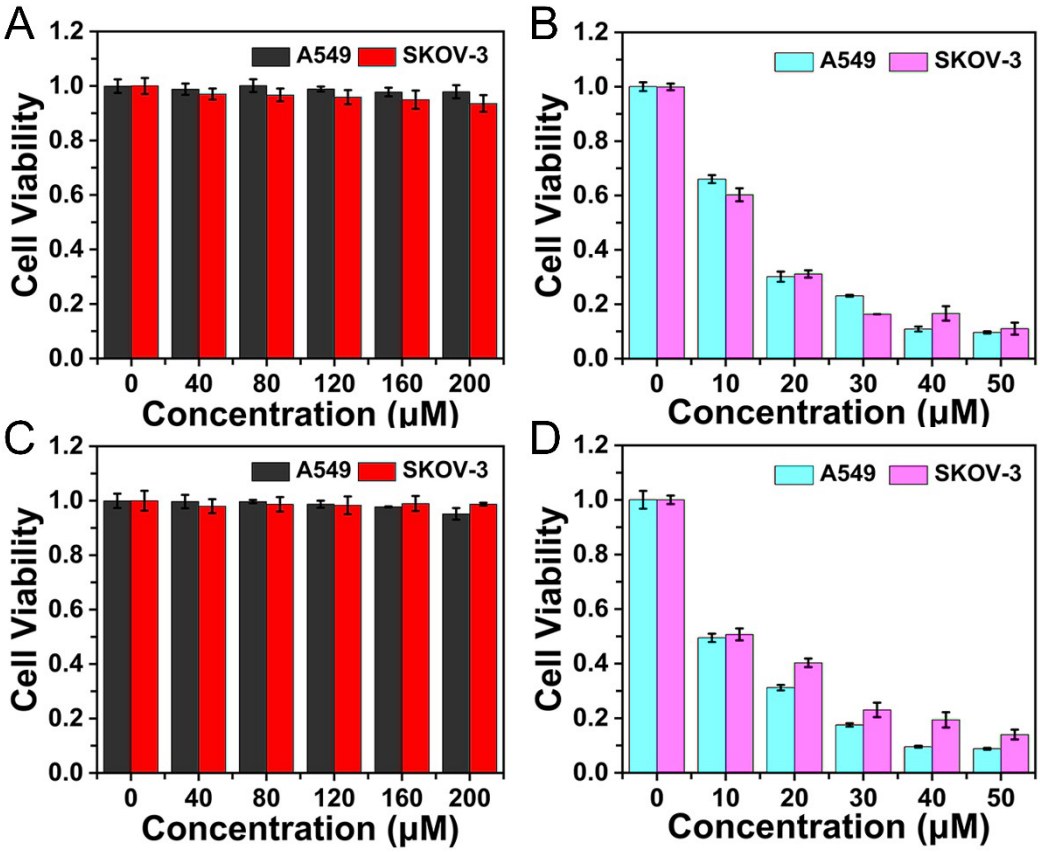

Fig. S36 Cell viability of A549 and SKOV-3 treated with **Ru-3** (A, B) and **Ru-4** (C, D) in the dark (A, C) or upon irradiation (B, D) for 30 min (470 nm, 40.5 J/cm^2).

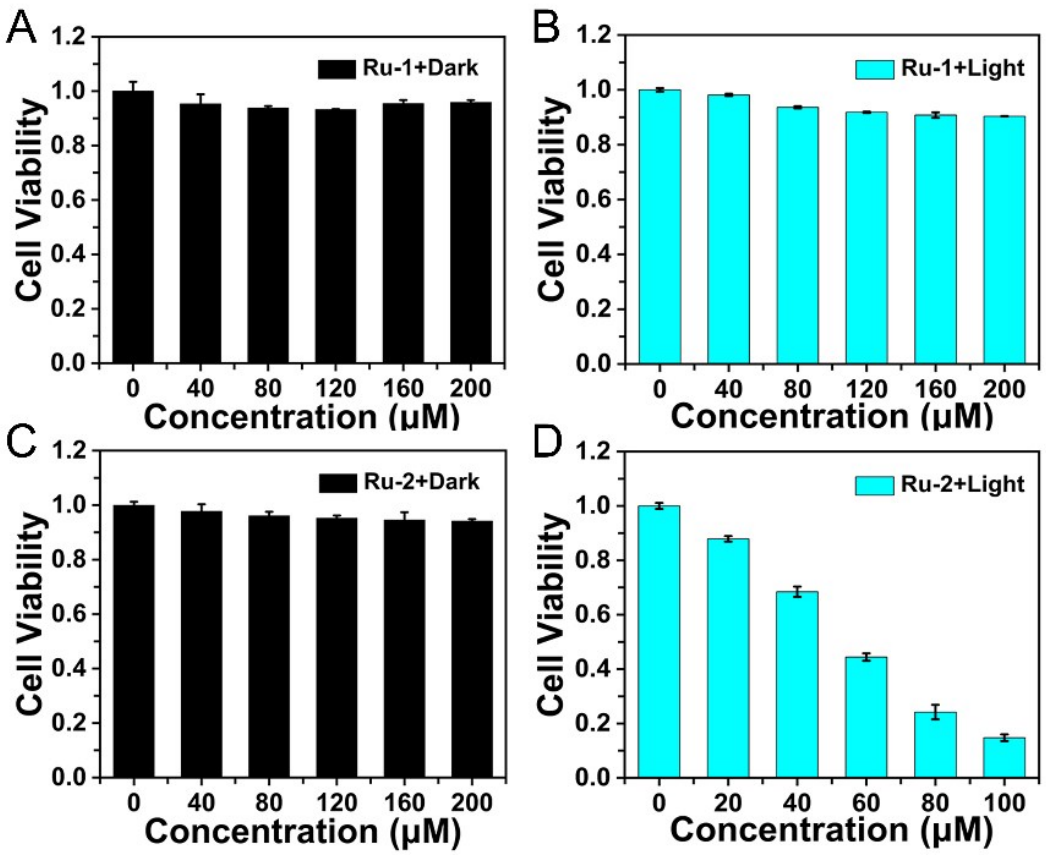

Fig. S37 Cell viability of A549/DDP treated with **Ru-1** (A, B) and **Ru-2** (C, D) in the dark (A, C) or upon irradiation (B, D) for 30 min (470 nm, 40.5 J/cm^2).

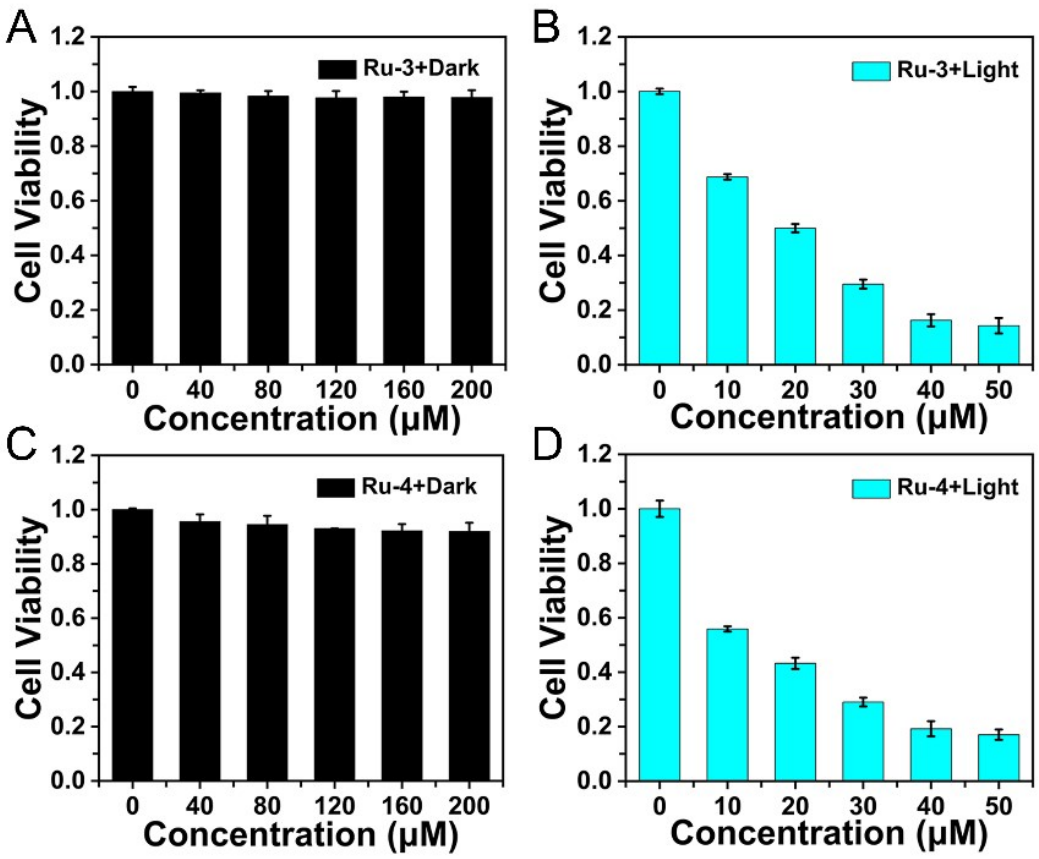

Fig. S38 Cell viability of A549/DDP treated with **Ru-3** (A, B) and **Ru-4** (C, D) in the dark (A, C) or upon irradiation (B, D) for 30 min (470 nm, 40.5 J/cm^2).

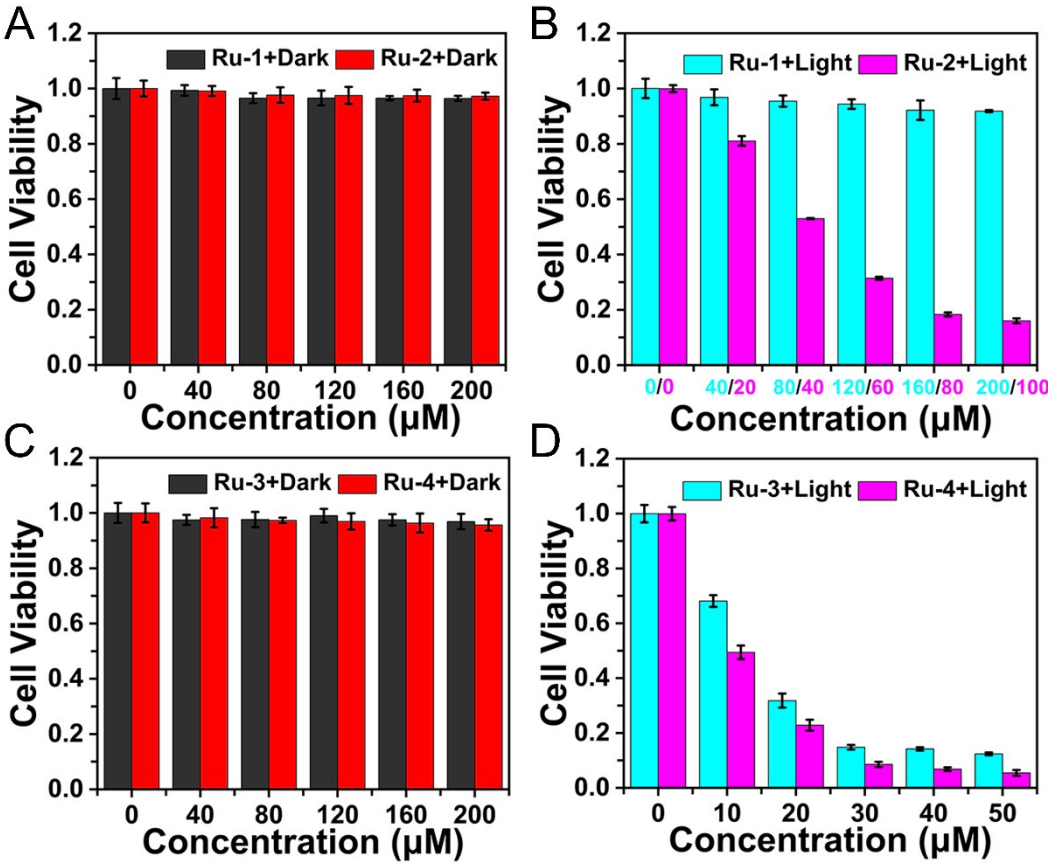

Fig. S39 Cell viability of A549 under hypoxic conditions (3% O_2) treated with **Ru-1, Ru-2** (A, B) and **Ru-3, Ru-4** (C, D) in the dark (A, C) or upon irradiation (B, D) for 30 min (470 nm, 40.5 J/cm^2).

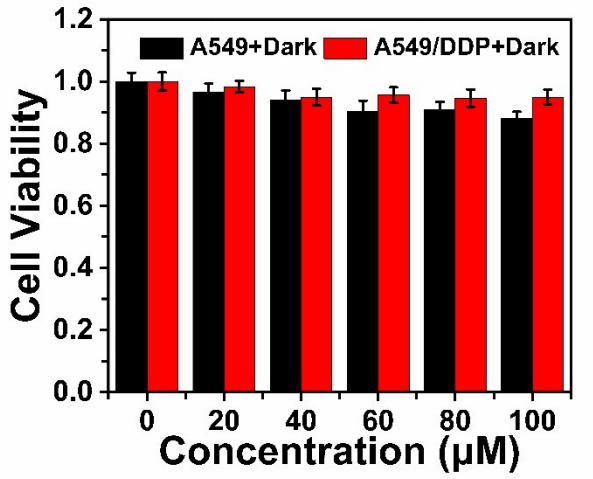

Fig. S40 Cell viability of A549 and A549/DDP treated with cisplatin in the dark.

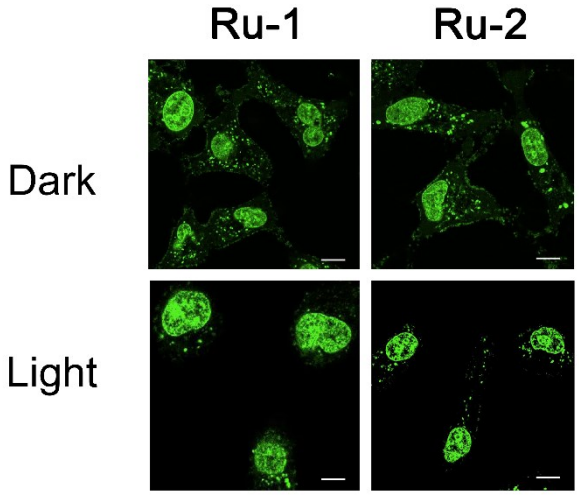

Fig. S41 A549 cells treated with **Ru-1** (left) and **Ru-2** (right) in the dark or upon irradiation (470 nm, 40.5 J/cm^2 for 30 min), and stained by PicoGreen. Scale bars: 10 μm.

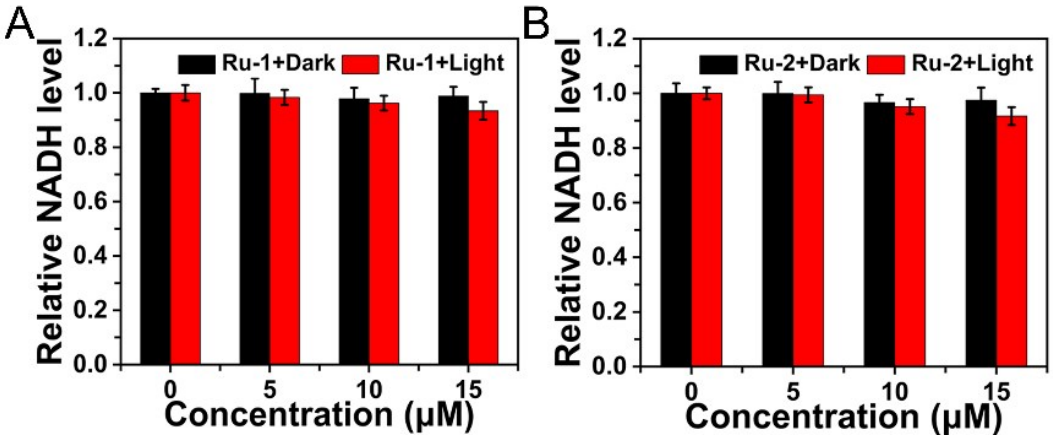

Fig. S42 Intracellular NADH levels of A549 cells treated with **Ru-1** (A) or **Ru-2** (B) in the dark or upon irradiation for 30 min (470 nm, 40.5 J/cm^2).

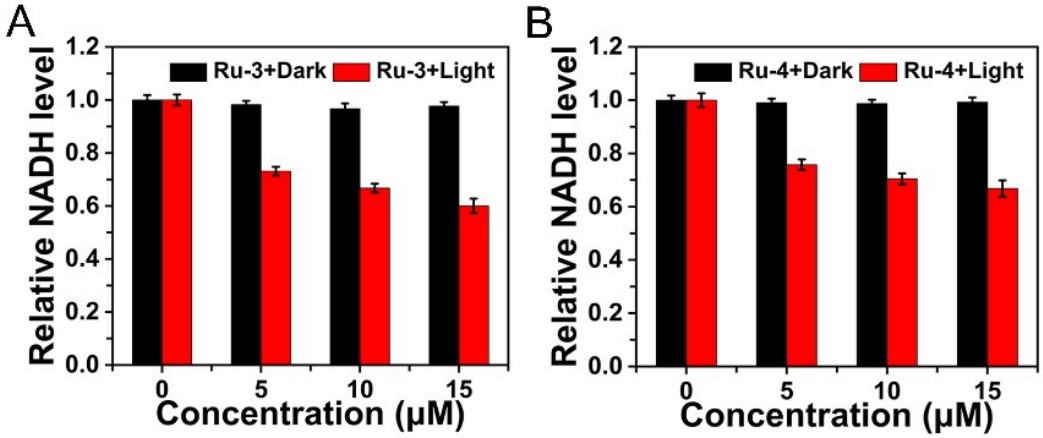

Fig. S43 Intracellular NADH levels of A549 cells under hypoxic conditions (3% O_2) treated with **Ru-3** (A) or **Ru-4** (B) in the dark or upon irradiation for 30 min (470 nm, 40.5 J/cm^2).

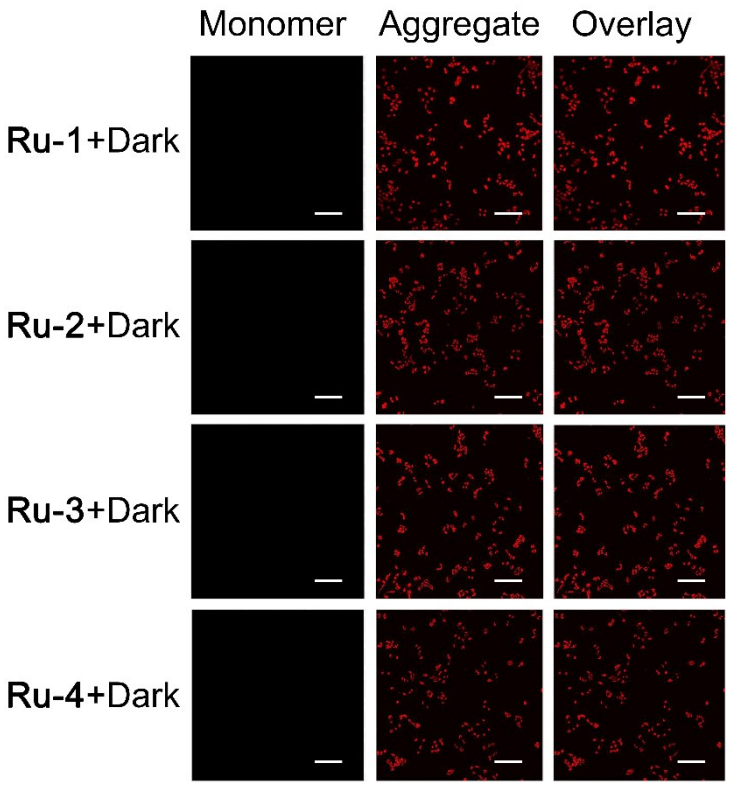

Fig. S44 Confocal luminescence images of JC-1 stained A549 cells after treatment with **Ru-1**-**Ru-4** (20 μM) in the dark. Scale bars: 200 μm.

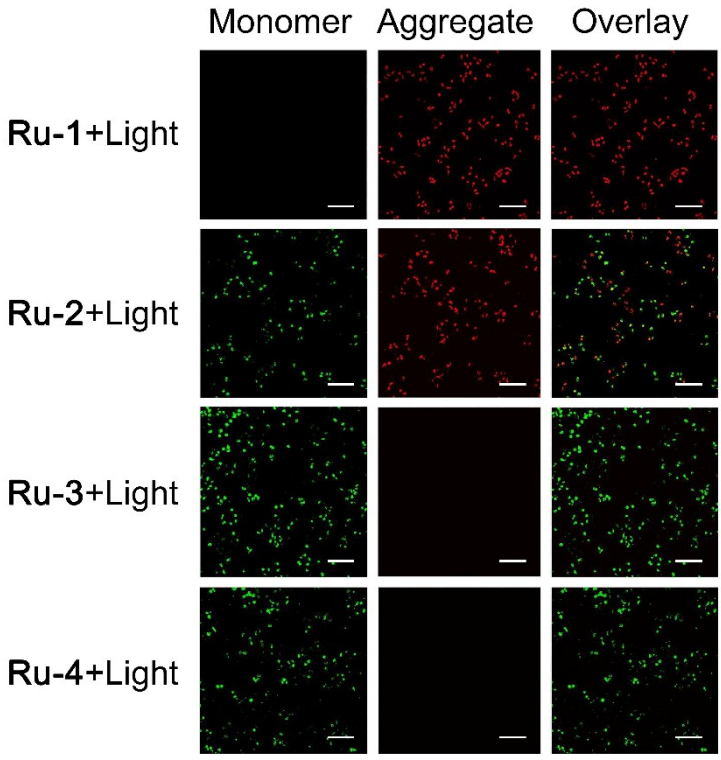

Fig. S45 Confocal luminescence images of JC-1 stained A549 cells after treatment with **Ru-1**-**Ru-4** (20 μM) upon irradiated for 30 min (470 nm, 40.5 J/cm^2). Scale bars: 200 μm.

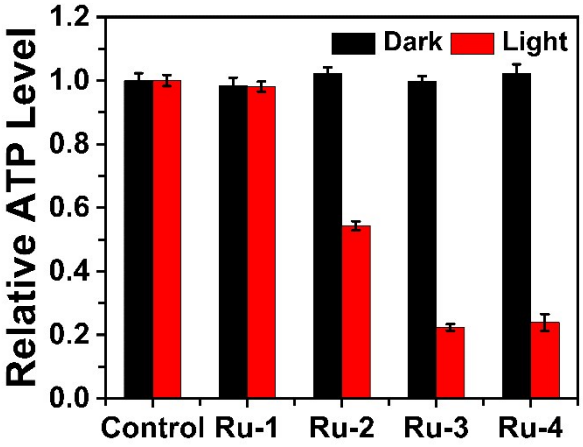

Fig. S46 Intracellular ATP levels of A549 cells treated with **Ru-1**-**Ru-4** in the dark or upon irradiation for 30 min (470 nm, 40.5 J/cm^2).

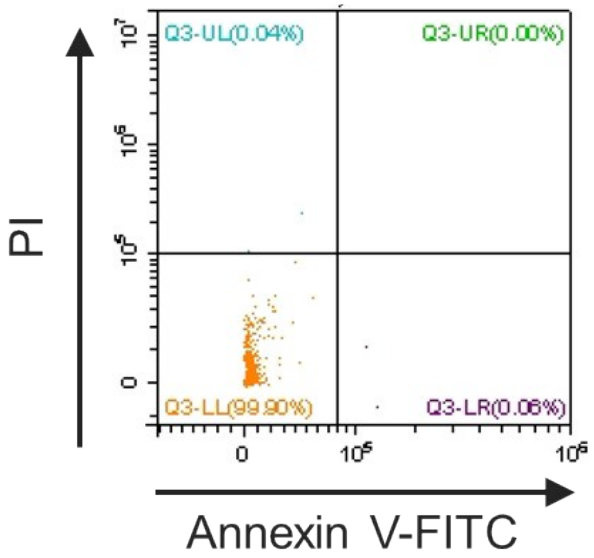

Fig. S47 Percentage of apoptotic A549 cells analyzed by flow cytometry treated only by irradiation (470 nm, 40.5 J/cm^2, 30 min).

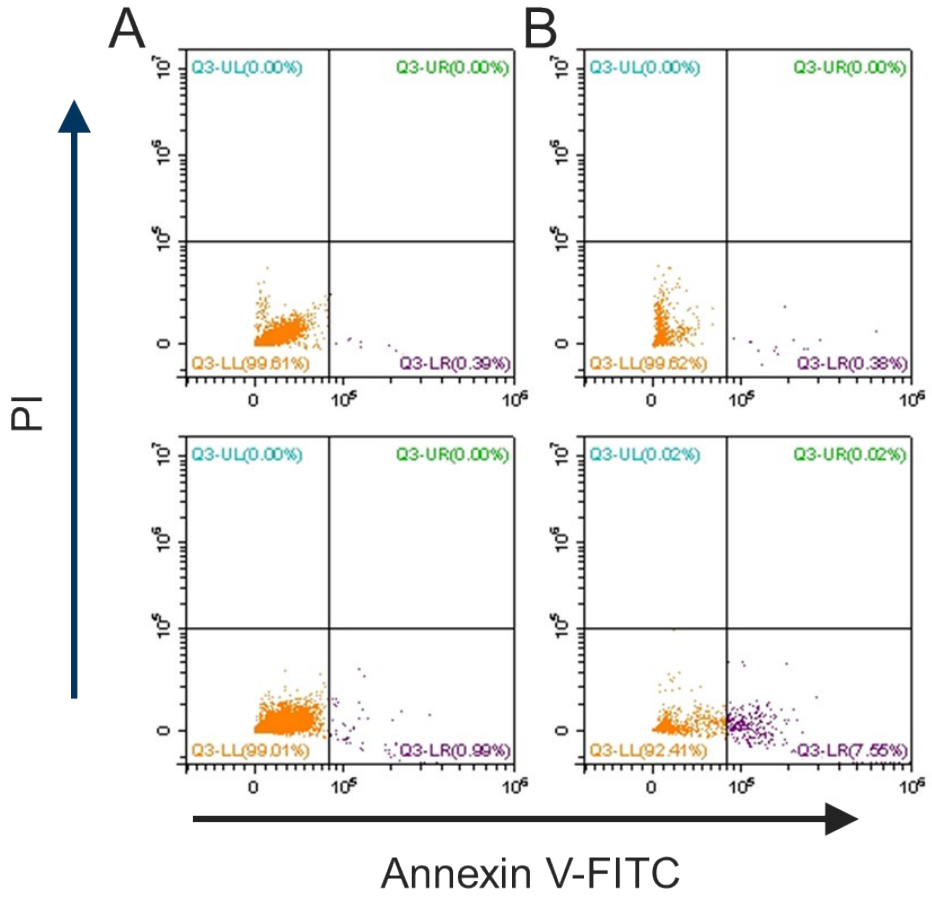

Fig. S48 Percentage of apoptotic A549 cells treated with **Ru-1** (A) and **Ru-2** (B) (10 μM) and analyzed by flow cytometry. A549 cells were kept in the dark (top) or irradiated for 30 min (470 nm, 40.5 J/cm^2) (bottom), then incubated for another 10 h in the dark.

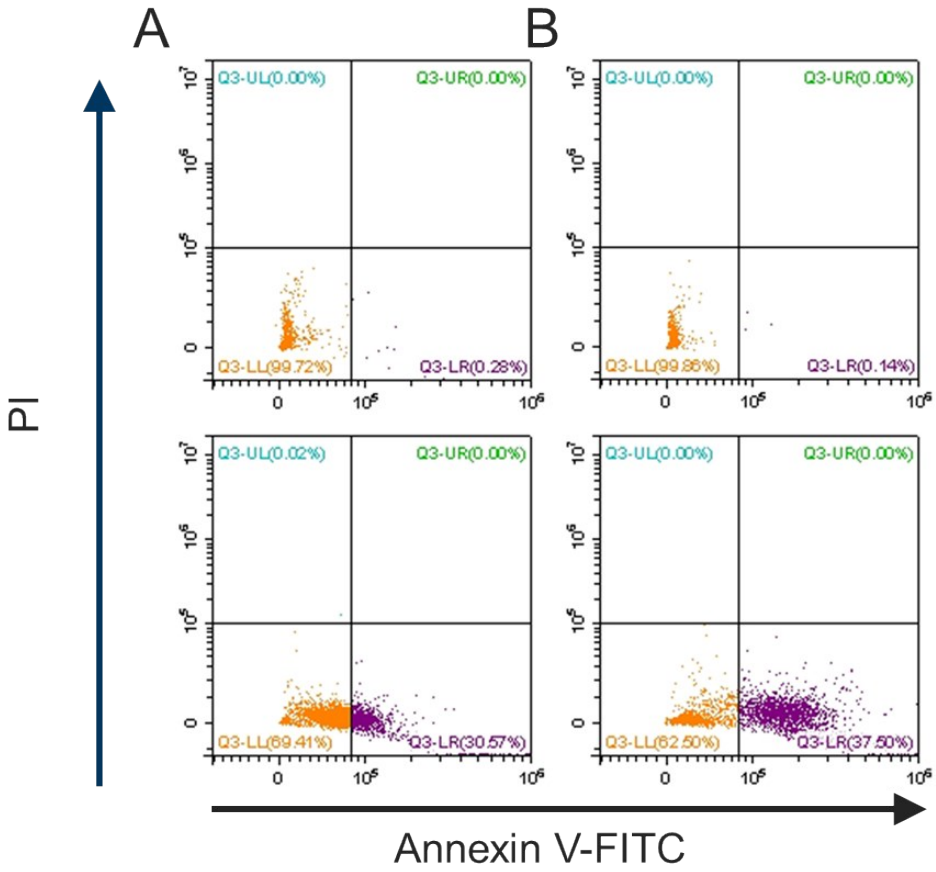

Fig. S49 Percentage of apoptotic A549 cells treated with **Ru-3** (A) and **Ru-4** (B) (10 μM) and analyzed by flow cytometry. A549 cells were kept in the dark (top) or irradiated for 30 min (470 nm, 40.5 J/cm^2) (bottom), then incubated for another 10 h in the dark.

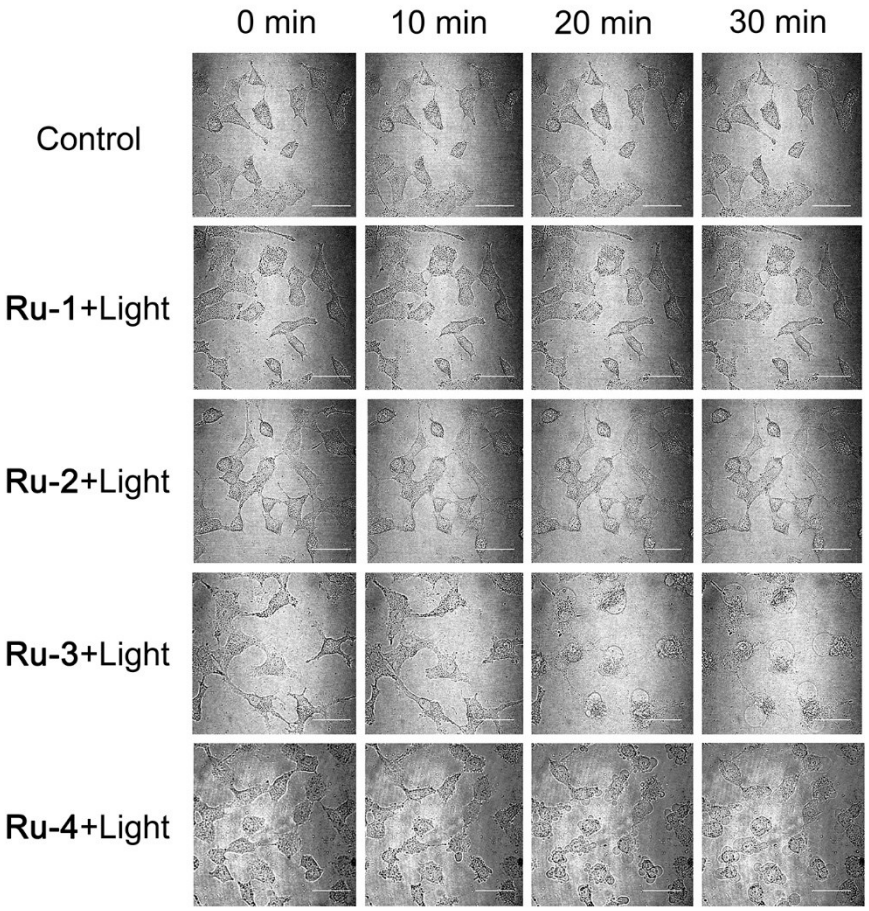

Fig. S50 Confocal microscopy images of A549 cells treated by **Ru-1**-**Ru-4** and two-photon irradiation (840 nm, 1.11 W/cm^2) equipped in the confocal microscopy at different times. The control group was treated only by irradiation (840 nm, 1.11 W/cm^2). Scale bars: 50 μm.

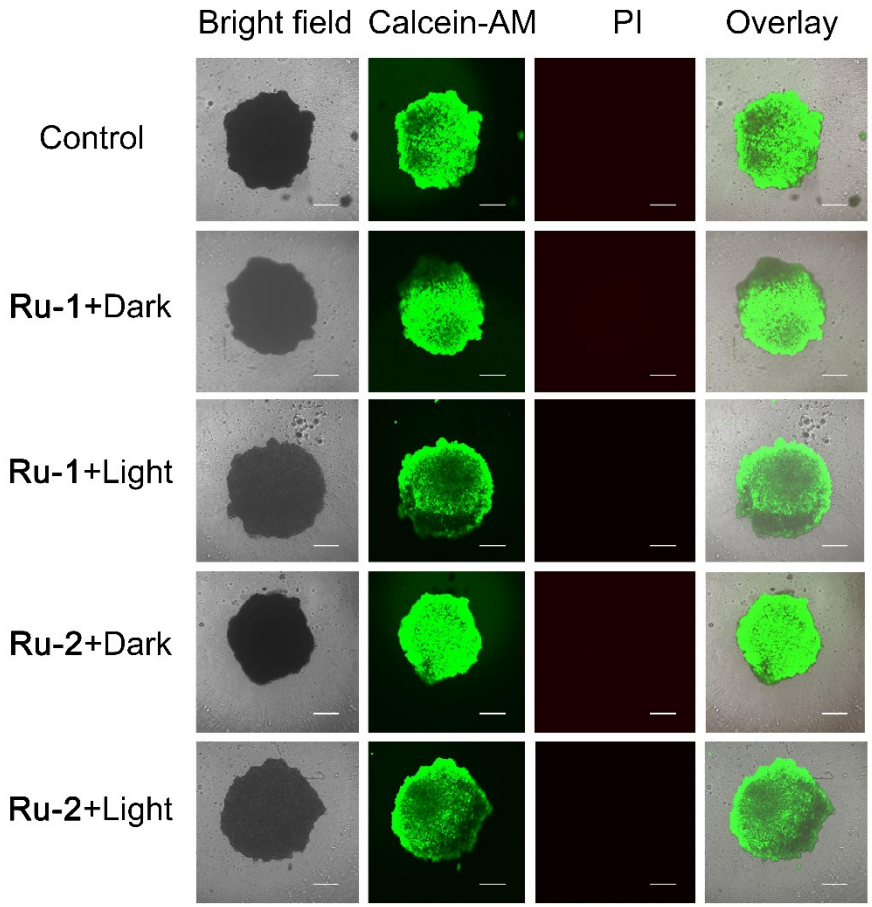

Fig. S51 Images of A549/DDP 3D MCSs treated by **Ru-1** or **Ru-2** (20 μM) with or without two-photon irradiation (800 nm, 1 W/cm^2) for 30 min and stained by Calcein-AM and PI. The control group was treated only by irradiation (800 nm, 1 W/cm^2). Scale bars: 200 μm.

Table S1 DNA binding constants, oil/water partition coefficients, relative quantum yields of ligand photo-dissociation, and reversible oxidation potentials of **Ru-1**-**Ru-4**.

	Ru-1	**Ru-2**	**Ru-3**	**Ru-4**
K (10^6 M^{-1}) [a]	0.40	0.60	0.87	1.66
Log $P_{o/w}$ [b]	-1.63	-1.11	-0.72	-0.44
Φ [c]	1.00	0.99	0.48	0.23
E(ox)[d] [V] (*vs* SCE)	1.33 (14)	1.32 (61)	1.31 (80)	1.30 (98)

[a] DNA binding constants obtained by DNA titration; [b] Logarithmic values of *n*-octanol/water partition coefficients; [c] Relative ligand-dissociation quantum yields vs. **Ru-1** upon 470 nm light irradiation. [d] Reversible half-wave oxidation potentials in N_2-saturated CH_3CN, peak separations are presented in mV in the parentheses.

Table S2. IC_{50} values (μM) of **Ru-1** and **Ru-2** towards different cell lines.

		A549	SKOV-3	A549 (Hypoxia, 3% O_2)	A549/DDP
Ru-1	Dark	> 200	> 200	> 200	> 200
	Light [a]	> 200	> 200	> 200	> 200
	PI [b]	- [c]	-	-	-
Ru-2	Dark	> 200	> 200	> 200	> 200
	Light	38.8 ± 0.2	45.9 ± 0.7	46.2 ± 0.4	54.1 ± 0.6
	PI	> 5	> 4	> 4	> 4

[a] Upon irradiation with a 470 nm LED lamp (40.5 J/cm^2) for 30 min; [b] PI = $IC_{50}^{dark}/IC_{50}^{light}$; [c] - means not measured.

Table S3. IC_{50} values (μM) of **Ru-3**, **Ru-4** and **Cisplatin** towards different cell lines.

		A549	SKOV-3	A549 (Hypoxia, 3% O_2)	A549/DDP
Ru-3	Dark	> 200	> 200	> 200	> 200
	Light [a]	14.2 ± 0.4	13.8 ± 0.3	14.7 ± 0.9	20.4 ± 1.1
	PI [b]	> 14	> 14	> 14	> 10
Ru-4	Dark	> 200	> 200	> 200	> 200
	Light	11.4 ± 0.5	12.6 ± 0.2	10.8 ± 1.5	14.7 ± 0.5
	PI	> 18	> 16	> 19	> 14
Cisplatin	Dark	> 100	- [c]	-	> 100

[a] Upon irradiation with a 470 nm LED lamp (40.5 J/cm^2) for 30 min; [b] PI = $IC_{50}^{dark}/IC_{50}^{light}$; [c] - means not measured.

References

1. M. T. Carter, M. Rodriguez, A. J. Bard, *J. Am. Chem. Soc*. 1989, **111**, 8901-8911.
2. C. Zhang, R. Guan, X. Liao, C. Ouyang, T.W. Rees, J. Liu, Y. Chen, L. Jia, Hui Chao, *Chem. Commun.*, 2019, **55**, 12547-12550.
3. M. Li, J. W. Y. Lam, F. Mahtab, S. Chen, W. Zhang, Y. Hong, J. Xiong, Q. Zheng and B. Z. Tang, *J. Mater. Chem. B*, 2013, **1**, 676-684.
4. L. He, M. Fei, J. Chen, Y. Tian, Y. Jiang, Y. Huang, K. Xu, J. Hu, Z. Zhao, Q. Zhang, H. Ni, L. Chen, *Mater. Today*, 2019, **22**, 76-84.
5. C. Xu, W. W. Webb, *J. Opt. Soc. Am. B: Opt. Phys.*, 1996, **13**, 481-491.
6. J. S. Basuki, H. T. T. Duong, A. Macmillan, R. B. Erlich, L. Esser, M. C. Akerfeldt, R. M. Whan, M. Kavallaris, C. Boyer, and T. P. Davis, *ACS Nano*, 2013, **7**, 10175-10189.
7. X. Liu, N. Liu, Y. Deng, S. Wang, T. Liu, Y. Tang, Y. Chen, and J. Lu, *Inorg. Chem.,* 2019, **58**, 16326-16329.
8. J. Chen, Y. Zhang, G. Li, F. Peng, X. Jie, J. She, G. Dongye, Z. Zou, S. Rong, L. Chen, *J. Biol. Inorg. Chem.*, 2018, **23**, 261-275.
9. H. Huang, Z. Li, Z. Liang, J. Yao, Y. Liu, *Eur. J. Med. Chem.*, 2011, **46**, 3282-3290.